



UNIVERSITY OF LEEDS

This is a repository copy of *Metalloaminopeptidases of the Protozoan Parasite Plasmodium falciparum as Targets for the Discovery of Novel Antimalarial Drugs*.

White Rose Research Online URL for this paper:  
<https://eprints.whiterose.ac.uk/170855/>

Version: Accepted Version

---

**Article:**

Mills, B, Isaac, RE [orcid.org/0000-0003-4792-6559](https://orcid.org/0000-0003-4792-6559) and Foster, R [orcid.org/0000-0002-2361-3884](https://orcid.org/0000-0002-2361-3884) (2021) Metalloaminopeptidases of the Protozoan Parasite Plasmodium falciparum as Targets for the Discovery of Novel Antimalarial Drugs. *Journal of Medicinal Chemistry*. ISSN 0022-2623

<https://doi.org/10.1021/acs.jmedchem.0c01721>

---

© 2021 American Chemical Society. This is an author produced version of a review published in the *Journal of Medicinal Chemistry*. Uploaded in accordance with the publisher's self-archiving policy.

**Reuse**

Items deposited in White Rose Research Online are protected by copyright, with all rights reserved unless indicated otherwise. They may be downloaded and/or printed for private study, or other acts as permitted by national copyright laws. The publisher or other rights holders may allow further reproduction and re-use of the full text version. This is indicated by the licence information on the White Rose Research Online record for the item.

**Takedown**

If you consider content in White Rose Research Online to be in breach of UK law, please notify us by emailing [eprints@whiterose.ac.uk](mailto:eprints@whiterose.ac.uk) including the URL of the record and the reason for the withdrawal request.



[eprints@whiterose.ac.uk](mailto:eprints@whiterose.ac.uk)  
<https://eprints.whiterose.ac.uk/>

# The metalloaminopeptidases of the protozoan parasite *Plasmodium falciparum* as targets for the discovery of novel antimalarial drugs.

*Belinda Mills, R. Elwyn Isaac, Richard Foster\**.

School of Chemistry and School of Biology, University of Leeds, Leeds, UK, LS2 9JT.

## ABSTRACT

Malaria poses a significant threat to approximately half of the world's population with an annual death toll close to half a million. The emergence of resistance to front-line antimalarials in the most lethal human parasite species, *Plasmodium falciparum* (*Pf*), threatens progress made in malaria control. The prospect of losing the efficacy of antimalarial drugs is driving the search for small molecules with new modes of action. Asexual reproduction of the parasite is critically dependant on the recycling of amino acids through catabolism of hemoglobin (Hb), which makes metalloaminopeptidases (MAPs) attractive targets for the development of new drugs. The *Pf* genome encodes eight MAPs, some of which have been found to be essential for parasite survival. In this article, we discuss the biological structure and function of each MAP within the *Pf* genome, along with the drug discovery efforts that have been undertaken to identify novel antimalarial candidates of therapeutic value.

## Introduction

Malaria, the world's most prevalent parasitic disease to affect humans poses a significant threat to millions of people across the globe every year. In 2019, it is estimated the number of malaria cases exceeded 220 million and that around 400,000 deaths from malaria occurred during this period, mostly children in Africa.<sup>1,2</sup> Human malaria is caused by one of five *Plasmodium* species (*P. falciparum*, *P. vivax* (*Pv*), *P. ovale*, *P. malariae* and *P. knowlesi*), the most common being *Pf* and is transmitted from person to person by blood-feeding Anopheles mosquitoes. In the absence of a vaccine, current measures to reduce the burden of malaria rely heavily on the administration of anti-malarial drugs and on vector control by eliminating aquatic breeding sites and the use of insecticides to prevent infection from biting adult females. The wide-spread use of chemical interventions over many years has resulted in the emergence of resistant populations of both parasite and vector.<sup>3</sup>

## Drug resistance

The evolution of drug resistance in the most clinically significant parasites, *P. falciparum* and *P. vivax*, threatens global efforts to control and eliminate malaria. Although the exact mechanisms by which the parasites acquire resistance to current drugs remains largely unknown, some genes have been noted as having an impact on the emergence of resistance.<sup>4</sup> Mutations in genes such as *Plasmodium falciparum* multidrug resistance 1 (*Pfmdr1*), *Pf* chloroquine resistance transporter (*PfCRT*), cytochrome *b* gene, dihydrofolate reductase and dihydropteroate synthase have all been identified as causing resistance to different classes of antimalarial drugs.<sup>5-9</sup> Chloroquine (CQ) was widely used in the treatment of all malaria until the 1960s when resistance in *Pf* parasites first emerged.<sup>10,11</sup> It wasn't until almost 30 years later that CQ resistance was identified in *P. vivax*

populations.<sup>12</sup> CQ is now rarely used for the treatment of *P. falciparum* malaria and artemisinin-based combination therapy (ACT) is now preferred.<sup>13,14</sup> However, CQ remains the preferred treatment for *P. vivax* malaria in most countries; in countries where CQ resistance is high, ACT is recommended.<sup>14-16</sup> Unfortunately, resistance to the most effective and widely used drug to treat *P. falciparum* malaria, artemisinin, has now emerged, and spread, in areas of south-east Asia, increasing the burden of malaria and highlighting the importance of developing novel antimalarial drugs which act through alternative pathways than those already targeted to reduce the risk of cross-resistance.<sup>13,17</sup>

In parallel to the development of novel antimalarials, ongoing research into the development of a malaria vaccine is also crucial to control the disease. The RTS,S malaria vaccine is the most clinically advanced vaccine to date, and the first to have undergone phase III clinical trials. It was first produced in 1987 by researchers at GlaxoSmithKline (GSK) in collaboration with researchers from the Walter Reed Army Institute of Research (WRAIR).<sup>18</sup> The RTS,S vaccine targets sporozoites and so is considered a pre-erythrocytic vaccine. Phase I and II clinical trials found that it was able to partially protect children and infants in Africa against malaria.<sup>19-21</sup> Phase III clinical trials took place from 2009-2014, and were focused on studying the long-term efficacy of the vaccine. The final study results concluded that a 3-dose RTS,S vaccination program reduced cases of clinical malaria in young children by 28% and in infants by 18%.<sup>22</sup> It was also found that cases were reduced further where a booster vaccination of RTS,S was administered 18 months after the first 3 doses.<sup>22</sup> Safety of the vaccine was also closely monitored and was found to be largely acceptable. Increased risk of febrile seizures and potential increased risk of meningitis were noted and these will need to be continually monitored as the vaccine progresses.<sup>22</sup> Whilst these results are promising for the implementation of a vaccine across the countries heavily affected by malaria,

it is still unknown if the WHO will implement policy for the use of the RTS,S vaccine and so continued development of antimalarial drugs remains of paramount importance.

#### Life cycle of *Plasmodium falciparum*

The *Pf* life cycle involves an asexual phase within the human host, followed by the sexual phase within the female Anopheles mosquito vector. This complex cycle can be split into three main stages: the sporogonic cycle within mosquitoes, the human liver stage, and the human erythrocytic stage.<sup>2,4,23,24</sup>

The life cycle begins when an infected mosquito bites a human and *Pf* parasites are injected into the skin.<sup>2</sup> The parasites then find their way into the bloodstream and are transported to the liver to begin the liver stage of their development. This whole liver stage (sometimes termed the pre-erythrocytic phase) lasts on average 5-6 days for *Pf* parasites and results in no symptoms of infection in the human host.

Release of haploid merozoites from the liver into the blood leads to the infection of erythrocytes (red blood cells, RBCs), marking the beginning of the human blood stage (also known as the erythrocytic stage). The merozoite is contained within a parasitophorous vacuole (PV), separated from the erythrocyte cytoplasm.<sup>24</sup> Here, the parasite undergoes multiple erythrocytic cycles, which in *Pf* are repeated every 48 hours. During each cycle, the merozoites inside the RBCs multiply asexually and develop through the ring stage trophozoites, mature trophozoites and into schizonts. The erythrocytic cycle begins again when the schizonts rupture, releasing more merozoites which can go on to infect more RBCs. Most parasites continue this cycle and infect more RBCs, however some of the merozoites are programmed to differentiate into male or female gametocytes. These gametocytes represent the sexual forms of the parasite and continue to circulate in the host bloodstream.

The sexual phase of the parasite is termed sporogony and occurs within the mosquito vector after a blood meal from an infected human is taken.<sup>2</sup> The gametocytes undergo sexual maturation and develop into zygotes that travel to the mosquito midgut wall to form oocysts. Rupture of the oocyst releases thousands of active sporozoites into the mosquito, and these then infect the insect's salivary glands. When the infected mosquito takes its next blood meal, these sporozoites are injected into another human host, beginning the life cycle again.

### Hemoglobin degradation

Due to the complex, yet well-studied, lifecycle of the *Pf* parasite there are various critical processes which can be targeted and exploited for the development of new antimalarial drugs. One of these processes which could potentially be targeted is the degradation of host Hb during the mature trophozoite phase of the erythrocytic stage. *Pf* parasites do not possess the ability to synthesize their own amino acids, and so they rely on the digestion of host Hb in order to obtain the amino acids required for growth and development.<sup>25</sup> Erythrocyte cytoplasmic proteins, mainly Hb, are ingested by the parasite *via* endocytosis and broken down to constituent amino acids in both the cytosol and a specialized organelle, the food vacuole (FV). This organelle contains several proteases required for the efficient degradation of Hb and the re-cycling of amino acids for protein synthesis during parasite replication. The catabolism of Hb is believed to follow a semi-ordered process involving a cascade of proteases working cooperatively to cleave the Hb polypeptide sequentially into peptide fragments (Figure 1).

A group of aspartic proteases (plasmepsins) and cysteine proteases (falcipains) are essential for the initial digestion of the host Hb. Four out of the ten plasmepsins encoded within the *Pf* genome are known to be localized to the FV. These are *Pf*PM1, *Pf*PM2, *Pf*HAP (*Plasmodium falciparum* histoaspartic proteinase) and *Pf*PM4.<sup>26,27</sup> *Pf*PM1, *Pf*PM2 and *Pf*PM4 are members of the A1 family of aspartic proteases; *Pf*HAP has a similar active site structure but one of the catalytic Asp residues

is substituted with His.<sup>28</sup> Out of these four, *PfPM1* and *PfPM2* are able to initiate the cleavage of the Hb molecule between residues Phe33 and Leu34.<sup>29,30</sup> The  $\alpha$ 33–34 bond resides within a hinge region of the molecule, whereby cleavage results in the unravelling of the Hb which exposes the polypeptide to further endoproteolytic cleavage by four FV plasmepsins, along with the falcipains *PfFP-2*, *PfFP-2'* and *PfFP-3*, to further digest the large globin units into smaller polypeptides.<sup>31</sup> These polypeptide fragments of up to 20 amino acids in length are then hydrolyzed into short peptides of around 5-10 amino acids by the metalloprotease falcilysin.<sup>32</sup> Next, the *Plasmodium falciparum* dipeptidyl aminopeptidase 1 (*PfDPAP1*) cleaves dipeptides from the N-terminus of the short peptide chains.<sup>33,34</sup> Cleavage of the remaining short peptides into the constituent amino acids occurs by the action of eight MAPs found in two locations within the parasite, the FV and the cytoplasm. These aminopeptidases are responsible for the release of N-terminal amino acids from short peptide chains and were previously believed to reside and function only within the neutral environment of the cytoplasm.<sup>35</sup> However, two of these aminopeptidases, aminopeptidase P (*PfAPP*) and alanyl aminopeptidase (*PfA-M1*), have since been reported to also localize within the acidic FV and so can act directly upon any short peptide fragments that meet their respective specificities.<sup>36–39</sup> The remaining peptide fragments are exported out of the FV and into the parasite's cytoplasm where all eight MAPs are believed to work in unison to complete the degradation of the peptides to free amino acids.

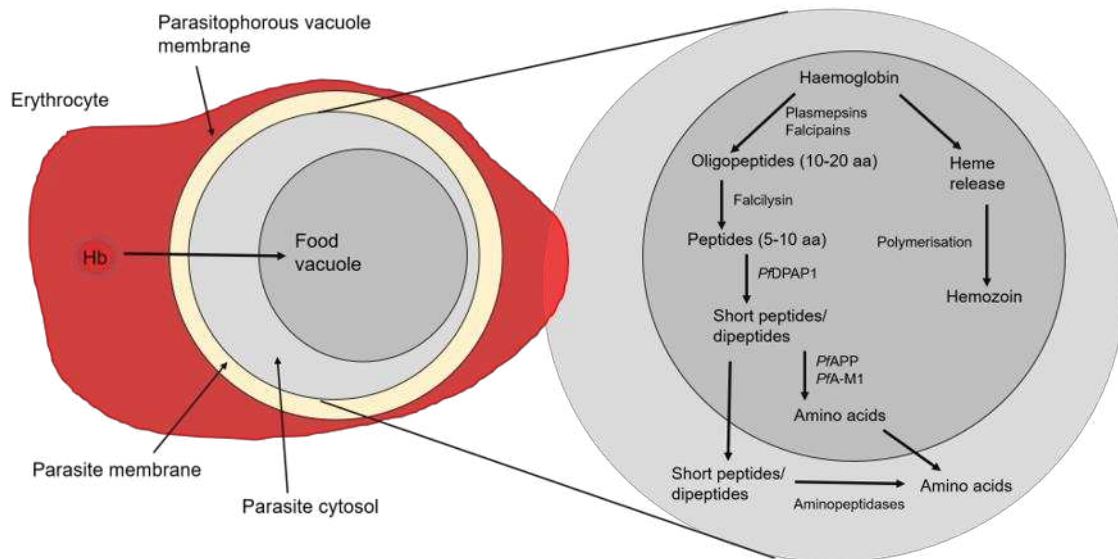


**Figure 1:** Schematic detailing the Hb degradation cascade within the *Pf* FV. Hb from the host cell cytoplasm is transported into the FV of the parasite. Here, endoproteases sequentially break down the Hb into successively smaller fragments, down to the constituent amino acids. Hb is initially cleaved at the hinge region by the plasmepsins and then further catabolized into oligopeptides, of around 10-20 residues in length, by the falcipains. Falcilysin then catabolizes these oligopeptides into shorter peptides of around 5-10 residues in length. The resultant peptides are then degraded into short peptides or dipeptides by dipeptidyl aminopeptidase 1 (*Pf*DPAP1), and these short peptides/dipeptides then undergo varying processes. Some of the short peptides/dipeptides are broken into constituent amino acids by MAPs found within the acidic FV (*Pf* aminopeptidase P (*Pf*APP) and *Pf* alanyl aminopeptidase (*Pf*A-M1)) whereas the rest are exported out of the FV and into the parasite's cytoplasm. Here, other MAPs catalyze the breakdown of the short peptides/dipeptides into individual amino acids, this time at neutral pH. Degradation of Hb by the plasmepsins also results in the release of toxic free heme. In order to protect itself from the build-up of heme, the parasite converts this free heme into hemozoin, also known as the malaria pigment.<sup>40,41</sup>

## Drug targets within the hemoglobin digestion pathway

Despite there being many proteases involved in the catalytic cascade of Hb degradation, only a few of these have been identified as being essential for parasite survival. The plasmepsins are responsible for the initial cleavage of the Hb molecule, but the high sequence similarity seen between all four enzymes (60-70%) suggests redundancy of each individual plasmepsin for *Pf* survival.<sup>42</sup> In addition, studies have shown that the falcipains exhibit a functional overlap with the plasmepsins, ensuring parasite survival even in the absence of all falcipain proteases.<sup>43</sup> This means that efforts to inhibit the early stages of Hb catabolism is likely to be challenging. At the other end of the digestive cascade, gene knockout studies have shown that some MAPs are vital for parasite survival and therefore attractive drug targets. Parasites with gene knockouts of *Pf* leucyl aminopeptidase (*PfA-M17*), *PfA-M1* and *PfAPP* were unable to be isolated, suggesting inhibition of these enzymes, either individually or in combination, would provide a therapeutic benefit in treating malaria infection.<sup>36,44</sup>

## Metalloaminopeptidases

MAPs are a group of ubiquitous exopeptidases that play an important role in the breakdown of peptides into their constituent amino acids through the cleavage of amino acid residues from the N-terminus. They are classed as metallo-enzymes because they contain one or two divalent metal ions within the active site which are critical for catalytic activity. Each of the MAPs also has a unique substrate specificity profile which is determined by the nature of the active site binding pockets (denoted as S<sub>1</sub>, S<sub>1</sub>', S<sub>2</sub>', etc., Figure 2).

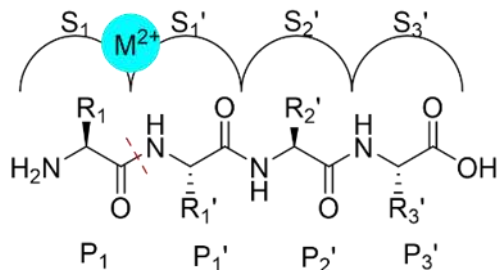


**Figure 2:** Schematic model of the MAPs active site. The residues of the tetrapeptide substrate (P<sub>1</sub>, P<sub>1</sub>', P<sub>2</sub>', P<sub>3</sub>') are situated relative to the corresponding enzyme sub-sites (S<sub>1</sub>, S<sub>1</sub>', S<sub>2</sub>', S<sub>3</sub>') using the nomenclature set out by Schechter and Berger.<sup>45</sup> A single catalytic divalent metal ion is shown in blue. The amide bond to be cleaved by the MAP, releasing the free N-terminal amino acid, is denoted by the red dashed line.

Within the *Pf* genome, eight MAPs have been identified: four methionine aminopeptidases (*PfMetAP1a*, *PfMetAP1b*, *PfMetAP1c*, and *PfMetAP2*); an alanyl aminopeptidases (*PfA-M1*); a leucyl aminopeptidase (*PfA-M17*); an aspartyl aminopeptidase (*PfM18AAP*); and an aminopeptidase P (*PfAPP*) (Table 1).<sup>46,47</sup> *Pf* parasites are also known to contain genetic information encoding a serine S33 prolyl iminopeptidase, *PfPAP*. This iminopeptidase is highly specific for the cleavage of N-terminal proline residues from short peptide chains and is present in a variety of organisms, however very little else is known about *PfPAP*.<sup>48–50</sup> In contrast, research into *Pv* is relatively limited and so there is little information available on the corresponding enzymes within this species. *Pf* and *Pv* are also considered biologically different to one another and so conclusions drawn for *Pf* may not be applicable to *P. vivax*.<sup>51</sup> Nonetheless, recent studies have begun to assess the potential for targeting the MAPs of *P. vivax* to provide cross-species inhibition, although a significant amount of further research is necessary to validate these enzymes.<sup>52,53</sup>

Each of the MAPs has a unique preference for the N-terminal amino acid being cleaved, suggesting a panel of enzymes with different substrate specificities function cooperatively for parasite survival. Experimental evidence for the essential nature of these enzymes for *Pf* parasite survival has led to recent interest in targeting them for the design and development of novel malarial therapeutics, although further evidence is required to confirm the validity of these enzymes as antimalarial targets.<sup>36,44</sup> Whilst the MAPs are proposed to play an important role in Hb degradation, it is thought that one or more of these enzymes may play additional roles within the parasite lifecycle.<sup>39</sup> For example, *PfA-M1* has been proven to function as a hemoglobinase but it has also been identified in *Pf* gametocytes, gametes and sporozoites, suggesting the biological role played by this enzyme is not limited to Hb degradation.<sup>38,39,54–56</sup> Herein we discuss the role that each of the metalloaminopeptidases play in the erythrocytic lifecycle of the *Pf* parasite and any developments which have been made in the drug discovery process with the aim of identifying a new therapy to combat drug-resistant malaria. The validity of individual aminopeptidases as drug targets relies on genetic evidence and the effects of enzyme inhibitors on parasite development. Although many of the inhibitors are selective for a class of aminopeptidase, care must be exercised in the interpretation of these results since unknown off-target effects might contribute to parasite toxicity.

**Table 1:** Summary of the five most studied *Pf*MAPs.

	<b>UniProt accession number</b>	<b>Metal cofactor</b>	<b>Size</b>	<b>Substrate specificity</b>	<b>Human homologs</b>	<b>Localization</b>
<i>PfMetAP1b</i>	Q8IJP2	Physiological cofactor is unknown. Highest activity seen	59.7 kDa	N-terminal Met residues	HuMetAP1	Cytosol

		with Zn(II) and Co(II)				
<i>PfA-M1</i>	O96935	Zn(II)	122 kDa – processed into 96, 68 and 35 kDa forms	Hydrophobic and basic N- terminal residues	hAPN	Cytosol, FV and nucleus
<i>PfA-M17</i>	Q8IL11	Zn(II)	67.8 kDa	Hydrophobic N-terminal residues	hLAP3	Cytosol
<i>PfM18AAP</i>	Q8I2J3	Zn(II)	65 kDa	Acidic N- terminal residues	DNPEP	Cytosol
<i>PfAPP</i>	A0A144A2H0	Mn(II)	157 kDa	Peptides with a penultimate N-terminal Pro residue (i.e. Xaa- Pro)	hAPP1, hAPP2 and hAPP3	Cytosol and FV

### Methionine aminopeptidases

The co-translational removal of N-terminal Met initiator residues from proteins during synthesis is a highly conserved process across both prokaryotes and eukaryotes, and is essential for the correct folding and subsequent processing of proteins.<sup>23,57,58</sup> Methionine aminopeptidases (MetAPs), the enzymes responsible for performing this role, can be sub-classified into two categories depending on the absence (type I, MetAP1) or presence (type II, MetAP2) of a ~60 residue peptide insertion within the catalytic domain. In eukaryotes, an additional N-terminal domain is also observed in MetAP2.<sup>57</sup> The *Pf* genome encodes for four MetAPs: three MetAP1 isoforms (namely *PfMetAP1a*, *b* and *c*), and one MetAP2 isoform (*PfMetAP2*).<sup>46</sup> Microarray analysis to determine the temporal expression pattern of each of the enzymes suggests that

*PfMetAP1c* may perform a different function to the other isoforms; *PfMetAP1c* is expressed predominantly in late-stage intra-erythrocytic parasites, whereas the other three orthologs are expressed much earlier in the life cycle.<sup>59</sup> Besides this, little data has been collected for homologs *PfMetAP1a* and *c*.

The four *PfMetAPs* all contain the conserved catalytic domain at the core of their structures

#### *Type I*

The three *PfMetAP1* isoforms all adopt the canonical MetAP1 catalytic domain at the core of their structure (Figure 3). This region is extended in *PfMetAP1b* and *PfMetAP1c* by the addition of N- and C- terminal sequences and by peptides inserted into the catalytic domain. *PfMetAP1c* has an N-terminal signal peptide immediately followed by a transit peptide required for localization of the enzyme to the apicoplast.<sup>60</sup> *PfMetAP1c* also contains a ~210-residue insertion within the catalytic domain. *PfMetAP1b* shares the highest level of sequence homology with human and yeast MetAP1 and is the only *PfMetAP* with a solved high-resolution structure (PDB ID: 3S6B) and therefore is the most characterized of the four *PfMetAPs*.<sup>61</sup> As with the human and yeast proteins, the conserved zinc-finger motif was observed within *PfMetAP1b*. In comparison to the human ortholog, *PfMetAP1b* contains a 56-residue N-terminal extension (NTE) and a 10-residue extension at the C-terminus. All three *PfMetAP1* enzymes contain the conserved active site residues (two Asp, one His, two Glu) responsible for divalent metal coordination and catalytic activity.<sup>61</sup>

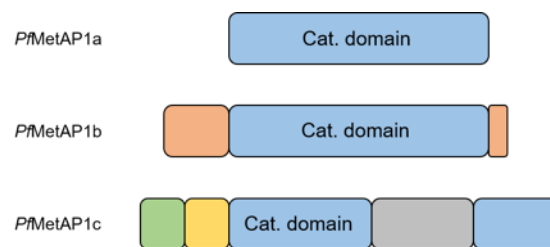


**Figure 3:** Schematic representation of the *Pf*MetAP1 domain structures. The conserved catalytic domain is shown in blue. The 56-residue NTE and 10-residue C-terminal extension of *Pf*MetAP1b are shown in pink. *Pf*MetAP1c contains an N-terminal signal peptide (shown in green) immediately followed by a transit peptide (shown in yellow) and a ~210-residue insertion within the catalytic domain.

#### *Type II*

*Pf*MetAP2 contains an N-terminal domain of 274 amino acids, followed by the conserved catalytic domain.<sup>60</sup> The five active site metal coordinating residues (two Asp, one His, two Glu) observed in all MetAP enzymes are also present in *Pf*MetAP2. *Pf*MetAP2 shares high C-terminal catalytic domain sequence identity (58%) with the human ortholog, HuMetAP2. The 64-residue catalytic domain insertion, the key characteristic in defining a type II MetAP, is also highly conserved between the human and malarial proteins. Despite these strong similarities, there are differences in the active site of the two enzymes, e.g. the absence of *Pf*MetAP2 residue Lys501 in HuMetAP2 which is believed to have a significant impact on the active site environment and might be exploited for the rational design of selective enzyme inhibitors. Additionally, *Pf*MetAP2 was found to contain multiple poly-asparagine sequences within the N-terminal domain: this is a characteristic of many malarial proteins.<sup>62</sup>

#### *Metal-ion content and pH stability*

Investigations into the optimum metal-ion cofactor and pH for enzyme activity were conducted using *Pf*MetAP1b.<sup>63</sup> Enzymatic activity was abolished on addition of the metal chelator, EDTA (5 mM), confirming the requirement of the metal ions for catalytic activity. The MetAP activity of the EDTA-treated apoenzyme at pH 7.5 was rescued by the addition of either Zn<sup>2+</sup>, Co<sup>2+</sup> or Mn<sup>2+</sup> to the assay buffer. The highest level of hydrolysis was recorded with Zn<sup>2+</sup> followed by Co<sup>2+</sup> and

then  $Mn^{2+}$ . Interestingly, the optimal concentration of  $Zn^{2+}$  and  $Mn^{2+}$  was 2  $\mu M$ , whereas activation by  $Co^{2+}$  ions occurred over a broad concentration range (1 to 500  $\mu M$ ).<sup>63</sup>

*PfMetAP1b* is highly specific for the cleavage of N-terminal Met residues

The enzymatic activity of *PfMetAP1b* against a library of 25 tetrapeptides with the structure Xaa-Gly-Met-Phe, where Xaa represents the 20 natural amino acids and 5 non-natural amino acids (norvaline, norleucine, ornithine, diaminobutyric acid, and diaminopropionic acid (DAP)) found that the only natural amino acid that *PfMetAP1b* could tolerate at the N-terminus was Met.<sup>63</sup> Catalytic activity was also observed for the substrates containing norvaline and norleucine in the N-terminal position and, interestingly, cleavage of norleucine was 60% more efficient when compared to Met.

Development of inhibitors towards the *PfMetAPs*

*Type I*

Following expression and purification of a recombinant form of the protein, a new family of *rPfMetAP1b* inhibitors containing the 2-(2-pyridinyl)-pyrimidine core was identified from a high-throughput screen (HTS) of 175,000 compounds.<sup>61</sup> Structure-activity relationship (SAR) data for 31 analogues, with differing substitutions around the pyrimidine core, led to the identification of XC11 (**1**, Figure 4) as a potent *rPfMetAP1b* inhibitor with an  $IC_{50}$  of 112 nM.<sup>61</sup> XC11 inhibited *in vitro* proliferation of the parasite at the erythrocytic ring stage of a CQ-sensitive (3D7) and a multidrug-resistant (Dd2) strain of *Pf* with  $IC_{50}$  values of 0.90 and 3.1  $\mu M$ , respectively.<sup>61</sup> Additionally, the inhibitor displayed >100-fold selectivity towards *rPfMetAP1b* over the other two *PfMetAP1* isozymes.<sup>61</sup> XC11 also displayed selectivity over the human version of the enzyme, with  $IC_{50}$  values of 0.7  $\mu M$  and 7  $\mu M$  for HuMetAP1 and HuMetAP2, respectively, and was not significantly toxic to cultured human fibroblasts.<sup>61</sup> The basis for the observed selectivity, however, is not known. Importantly, the *in vivo* antimalarial activity of XC11 was established using both

CQ-sensitive (*Plasmodium berghei*) and CQ-resistant (*Plasmodium yoelii*) mouse models. In both models, XC11 reduced parasitaemia and extended the mean survival time of the mice. XC11 administered twice a day at 20 mg/kg cured 60% of mice infected with the *P. berghei* species and 80% of the mice infected with the *P. yoelii* species.<sup>61</sup>

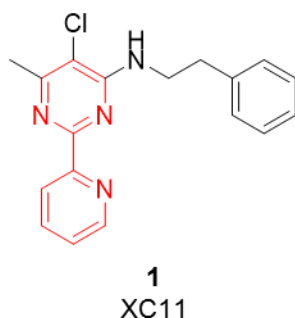


**Figure 4:** Potent *Pf*MetAP1b inhibitor, XC11. The 2-(2-pyridinyl)-pyrimidine core which is vital for activity is highlighted in red.<sup>61</sup>

This preliminary evidence all points to a promising new lead compound, which may have the potential to be further developed into a new class of antimalarial drug. Nonetheless, further investigations into the reasoning behind the observed selectivity would provide useful information for the future development of analogues. Despite XC11 being labelled as an important lead compound for the development of *Pf*MetAP1b inhibitors, no further studies have been published in recent years and so it appears that this enzyme is not being prioritized for inhibitor development.

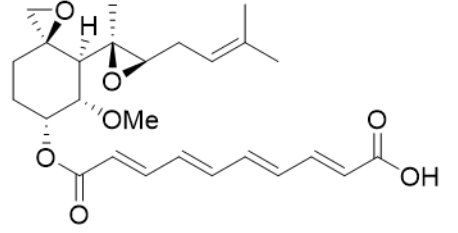
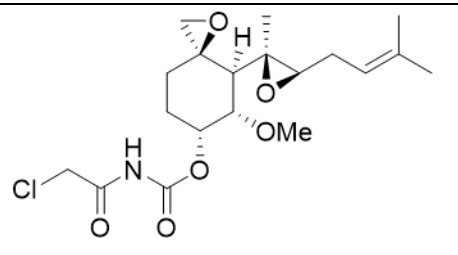
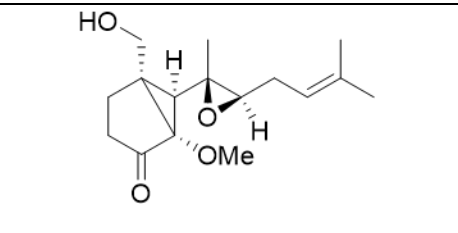
#### *Type II*

The antimalarial activity of MetAP2 inhibitors fumagillin (**2**) and TNP-470 (**3**) has been reported (Table 2).<sup>60</sup> Fumagillin, a natural product, and TNP-470, a synthetic derivate, covalently bind to an active site His residue of HuMetAP2, however fumagillin has been shown to bind reversibly to *Pf*MetAP2 despite the conservation of the active site His residue.<sup>60</sup> Both compounds potently block parasite growth of *in vitro* cultures of two different *Pf* strains, perhaps to an extent greater than

would be expected considering the low activity on r*Pf*MetAP2.<sup>60</sup> Whilst the authors provide evidence for a direct interaction between TNP-470 and *Pf*MetAP2, it may be that this interaction is not the only cause of parasite proliferation inhibition.<sup>60</sup> It has also been suggested that the higher cellular activity levels of these compounds in mammalian studies may be attributed to the reduced concentration of MetAP2 within the cellular environment compared to that required for *in vitro* enzymatic assays.<sup>64</sup> Additionally, fumagillin and TNP-470 are potent inhibitors of HuMetAP2, thus presenting issues surrounding selectivity.<sup>64</sup> Since these compounds are covalent inhibitors of HuMetAP2, measurement of the IC<sub>50</sub> values is challenging due to irreversible inhibition over a prolonged period.<sup>65</sup> Despite this, covalent inhibitors offer an advantage in that their high potencies allow for lower doses and higher drug efficiency, and irreversible binding offers the potential to reduce the development of resistance.<sup>66</sup> Additionally, the notion that covalent inhibitors offer poor selectivity is not always the case and so differences between the substrate binding sites of HuMetAP2 and *Pf*MetAP2 might be exploited to develop analogues of fumagillin which offer selectivity for inhibition of the malarial enzyme.<sup>60,64,66</sup>

**Table 2:** Structures of fumagillin and its derivatives active against MetAP2. IC<sub>50</sub> values against *Pf*MetAP2 were determined using the Dex-Fum-mediated mammalian three-hybrid assay. The effect of TNP-470 and fumarranol on proliferation of *Pf*NF54 and W2 strains *in vitro* were also measured.<sup>60</sup> Inhibition of human MetAP2 enzymatic activity was measured in a separate study.<sup>64</sup> N.D = Not determined.

<b>Compound</b>	<b>IC<sub>50</sub> r<i>Pf</i>MetAP2 (<math>\mu</math>M)</b>	<b>IC<sub>50</sub> HuMetAP2 (<math>\mu</math>M)</b>	<b>IC<sub>50</sub> <i>in vitro</i> (<math>\mu</math>M) (<i>Pf</i> strain)</b>
-----------------	---	---	---

2	Fumagillin		N.D	N.D	N.D
3	TNP-470		$2.0 \pm 1.0$	0.001	$0.002 \pm 0.0003$ (NF54) $0.003 \pm 0.0003$ (W2)
4	Fumarranol		$116 \pm 27$	3.23	$0.16 \pm 0.03$ (NF54) $0.27 \pm 0.07$ (W2)

More recently, the synthesis of analogues of fumagillin in order to reduce toxicity and improve pharmacokinetic (PK) properties has been investigated.<sup>64</sup> The most prominent analogue, fumarranol (**4**, see Table 2), was found to be a non-covalent HuMetAP2 inhibitor displaying reduced potency towards the human enzyme and lower toxicity in animal studies compared to TNP-470.<sup>64</sup> In addition to this, fumarranol was found to bind to *Pf*MetAP2, inhibit parasite growth *in vitro* and, more importantly, blocked *in vivo* parasite growth of a murine model.<sup>60</sup> In comparison to TNP-470, fumarranol was found to be ~80 times less potent towards *in vitro* cultures of both a CQ-sensitive (NF54) and a multidrug-resistant (W2) strain.<sup>60</sup> The same reduced potency was observed *in vivo*, however mice were able to tolerate a larger dose of fumarranol compared to TNP-470 which resulted in greater efficacy than TNP-470 overall for reducing parasitaemia.<sup>64</sup> Neither fumarranol nor TNP-470 had any effect on the activity of *Pf*MetAP1a, b or c, at a concentration of 300  $\mu$ M, indicating specificity towards the type II MetAP.<sup>60</sup> The preferential

toxicity profile of fumarranol has been highlighted as a lead candidate for future development into a potential antimalarial drug. However, future extensive work in fine tuning the selectivity of the inhibitor towards the malarial enzyme over the human ortholog would be required in order to reduce the risk of off-target host toxicity.

### Alanyl aminopeptidase

*PfA-M1* is a 122 kDa monomeric protein so named as it belongs to the M1 family of metalloproteases as defined by the active site structure.<sup>67,68</sup> It contains the four conserved M1 domains typical of all enzymes across the family along with a 194-residue NTE specific to the malarial protein.

*PfA-M1* contains the conserved structural features of the M1-family of aminopeptidases

The gene encoding for *PfA-M1* predicts a full-length protein of 122 kDa that is processed to smaller, catalytically active 96 and 68 kDa mature forms.<sup>68</sup> Further to this, a 35 kDa species has more recently been identified.<sup>69</sup> The 68 kDa species contains amino acid residues from domains I, II and III, but not the final 290 amino acids (domain IV) from the C-terminus. Conversely, the amino acids found in the 35 kDa species correspond to the 290 domain IV C-terminal residues. The two proteins appear to arise from proteolytic cleavage at residue Leu796, which lies between two domain IV  $\alpha$ -helices, and are thought to form a 68/35 active complex.<sup>69</sup>

### *X-ray crystal structure*

The X-ray crystal structure of recombinant (r) *PfA-M1* (residues 196-1085), expressed in *E. coli* without the 194 amino acid NTE, has been solved to 2.1 Å (PDB ID: 3EBG).<sup>70</sup> This truncated r*PfA-M1* construct was found to be both soluble and functional. More recently, truncated 3D structures of *PfA-M1* containing only one point mutation (PDB ID: 4J3B) and no mutations (PDB

ID: 6SBQ) compared to the native enzyme have been published.<sup>71,72</sup> The structure contains the aminopeptidase N-fold common to the M1-family of aminopeptidases, such as *E. coli* PepN and human aminopeptidase N (hAPN).<sup>70,73,74</sup> Comparison of the structures of *PfA*-M1 and *EcPepN* reveal a conserved four-domain structure, with overall 35% sequence identity (Table 3).<sup>75</sup> The 194-residue NTE of *PfA*-M1 is not found in the prokaryotic species and is thought to only be found in the corresponding aminopeptidases of other *Plasmodium* species.<sup>69,76</sup> The four domains consist of 26  $\alpha$ -helices and seven  $\beta$ -sheets.

**Table 3:** Sequence alignment of *PfA*-M1 (UniProtKB accession number– O96935), *EcPepN* (UniProtKB accession number – P04825) and hAPN (UniProtKB accession number – P15144).<sup>75</sup> The 194 residue NTE in *PfA*-M1 is highlighted in green. Conserved residues between the three sequences are colored red, non-conserved residues are colored in blue. The zinc-binding motif residues are shown in bold and highlighted on a yellow background. The GAMEN substrate specificity motif is highlighted on a black background.

<i>PfA</i> -M1	1	MKLTGKGCAYKYIIFTVLILANILYDNKKRCMIKKNLRISSCGIIISRLKSNNSYNSFNKNYNFTSAISELQFSNFWNLDI	80
<i>EcPepN</i>		-----	
hAPN	1	--MAKG-----FYISK-----SLGILGILG-----VAAVCTI-----I	27
<i>PfA</i> -M1	81	LQKDI FSNIHNNKPKQSYI IHKRLMSEKGDNNNNHQNNNNGDNNKRLGSSVNVNEENTCSDKRMKPFEEGHGITQVDKM	160
<i>EcPepN</i>		-----	
hAPN	28	ALSVVYS-----QEKNKNANSSPVASTTPSASATTNPA-----	60
<i>PfA</i> -M1	161	NNNSDHLQNGVMMNLNSNNVNNNNNSVVKNEPKIHYRKDYKPSGFTINNVTLNINIHNETIVRSVLDMDISKH--	238
<i>EcPepN</i>	1	-----MTQQPQAKYRHDYRAPDYQITDIDLTFDLDAQTVVTAV--SQAVRH--	45
hAPN	61	--SATTLDQSKAWN-----RYRLPNTLKPDSY---RVTLRPLYTPNDRGLYVFKGSSVTRFTC	113
<i>PfA</i> -M1	239	-NVGEDLVFDGVLKIN-----EISINNKLVGEEYTYDNEFLTIF--SKFVPKSKFASSE--VIIHPETNYA	303
<i>EcPepN</i>	46	-----SVHIND--EPWTAWKEEGALVIS--NLPE--RFTLKII--NEISPAANTA	105
hAPN	114	KEATDVI IHSKLLNYTLSQGRVVRVLRGVGSGSPDDIDKTELVEPTEYLVVHLKGLVKDSQYEMDSEFEGELADDLAGF	193
<i>PfA</i> -M1	304	LTGLYKSKN---IIVSQCEATGFRRIITFFIDRPMMAKYDVTVTADKEKYPVLLSNGDKVNEF---EIPGGRHGARFND	376
<i>EcPepN</i>	106	LEGLYQSGD---ALCTQCEAEGFRHITYYLDRPDMVLAFTTKIADKIKYPFLLSNGNRVAQG---ELENGRHWVQWQD	178
hAPN	194	YRSEYMEGNVRKVVATTQMQAADARKSFPCFDEPAMKAEFNITLIHP--KDLTALSMLPKGPSTPLPEDFNWVQTEFHT	271
<i>PfA</i> -M1	377	PHLKPCYLFVAVAGDLKLSATYITKYTKKVELYVFSSEKYVS--KLQWALECLKKSMAFDEDFYFGLYDLSRLNLVAV	454
<i>EcPepN</i>	179	PFPKPCYLFVAVAGDFDVLDRDTFTTR--SGREVALEYVDRGNLD--RAPWAMTSLKNSMKWDEERFGLYDLDIYMIVAV	255
hAPN	272	TPKMSTYLLAFIVSEFDYVEKQASNG-----VLIRIWARPSAIAAGHGDYALNVTGPILNFFAGHYDTPYPLPKSDQIGL	346
<i>PfA</i> -M1	455	SDFNVGAMENKGLNIFNANSLASKKNSIDFSYARILTVVGHYFNHTGNRVTLRDWFQTLTKGLTVHRENLFSEEMT	534
<i>EcPepN</i>	256	DFFNMGAMENKGLNIFNSKYVLARTDTATDKDYLDIERVIGHEYFNWNTGNRVTCRDWFQLSLKEGLTVFRDQEFSSDLG	335
hAPN	347	PDFNAGAMENGLVITYRENSLFDPLSSSSSNKERVVTVIAHELAHQWFGNLVTIEWWNLWLNEGFASYVEYLGADY--	424
<i>PfA</i> -M1	535	KTVTTRLSHVDLLR--SVQFLEDSSPLSHPIR--PESYVSM-----ENFYTTTVYDKGSEVMRMYLTIIGEEYKKGFDIY	606
<i>EcPepN</i>	336	SRAVNRINNVRTMR--GLQFAEDASPMAPHIR--PDMVIEM-----NNFYTLTVYKGAEVIRMIHTLLGEEFNFKGMQLY	407
hAPN	425	AEPFWNLKDLMLNLDVYRVMADVADALASSHPLSTPASEINTPAQISELFDFA--ISYKGSVLRMLSSFLSEDFVFKGLASY	503
<i>PfA</i> -M1	607	IKKNDGNTATCEDFNAYEQAYKMKKADNSANLNQYL--LWFSQSGTPHVSKFYNYDAEKKQYSIHVNQYTKPDENQKEKK	685
<i>EcPepN</i>	408	FERHDGSAATCDDFVQAMEDA-----SNVDLSHFR--RWYSQSGTPIVTVKDDYNPETEQYTLTISQRTPADPDQAEKQ	479
hAPN	504	LHTFAYNTIYLNLDLHLEAVNNRSTQLPTTVRDMNRWTLQMGFPVITVDTSTGTLSQEHFL-----LDDPNSVTRPS	578
<i>PfA</i> -M1	686	PLFIPISVGLINPENGKEMISQ-----TTLELTKESDTFVFNNAIVKPIPSLFRGFSAPVYIEDNLTDEERILLKYD	758
<i>EcPepN</i>	480	PLHIPFAIELEYDNE--GKVIPLQKGGHPVNSVLNVTQAEQTFVFDNVYFQVPALLCEFSAPVKLEYKWSDDQLTFLMRHA	558
hAPN	579	EFNYVWIVPITSIRDGRQQDYW-----LIDVRAQNDLFTSTSGNEVLLNLTGYRVNYDEENW-----RKI	642
<i>PfA</i> -M1	759	SDAFVRYNSCTNIYMKQILMNYNEFLKAKNEKLESFNLTPVNAQFIDAIKYLLEDPHADAGFKSYIVSLPQDRIYINQVVS	838
<i>EcPepN</i>	559	RNDFSRWDAAQSLLATYIKLNV-----ARHQGGQLSL--PVHVA--DAFRAVLLDEKIDPALAAEILTLPSPVNEMAELFD	630
hAPN	643	QTQLQRDHSIAIPVINRAQINDAFNLSAHHKVPVTLAL--NNTLF-----LIEERQYMPWEAALSLSYFKLMFDRSE	713

<i>PfA</i> -M1	839	NLDTDLVADTKEYIYKQIGDKLNDVYYKMPKSLKAKADDLTYFNDESHVDFDQMMRTRLRNTLLSLLSKAQYPNILNEII	918
<i>EcPepN</i>	631	IIDPIAIAEVREALTRTLATELAEDELLAIYNA-----NYQSEYRVEHEDIAKRTLNRNACLRFLAFGE--THLADVLV	700
<i>hAPN</i>	714	VYGP-----MKNYLKKQVTP-----LFIHFRN-----NTNNWREIPENLMDQYSEVNAISTACSNV-PECEEMVS	773
<i>PfA</i> -M1	919	EHSKSPYPSNWL-----SLSVSAYF---DKYFELYDKTYKLSKDDELLLQEWLKTVSRSDRDKDIYEILKKELENEVLKD	989
<i>EcPepN</i>	701	--SKQFHEANNMTDALAALSAAVAAQLPCRDALMQEYDDKWH---QNGLVMDKWFILQATSPAANVLETVRGLLQHRST	775
<i>hAPN</i>	774	GLFKQWMENPNNNPIHPNLRSTVYCNA-IAQGGEEWDFAWEQFRNATLVNEADKLRAALACSKELW-----ILNRYLSY	847
<i>PfA</i> -M1	990	SKNPNDIR-----AVYLPFT--NNLRR--FHDISGKGYKLIAEVIKTKDFNPMVATQLCEPFKLNWKL	1049
<i>EcPepN</i>	776	MSNPNRIR-----SLIGAFAGSNPAA--FHAEDGSGYLFVEMLTDLNSRNPQVASRLIEPLIRLKRY	836
<i>hAPN</i>	848	TLNPDILIRKQDATSTIISITNNVIGQLVWDFVQSNWKKLFNDYGGGFSFNSLIQAVTRRFSTEYELQQLQEQFKDNEE	927
<i>PfA</i> -M1	1050	DT--KRQELMLNEMNTMLQEPNISNNLKEYLLR--LTNKL-	1085
<i>EcPepN</i>	837	DA--KRQEKMRAALEQLKGLLENLSGDLYE---K-ITKALA	870
<i>hAPN</i>	928	TGFGSGTRALEQALEKTKANIKWVKENKEVVLLQWFTENSK	967

### Active site

The active site of *PfA*-M1 is located within domain II (residues 392–649) and is buried within a thermolysin-like fold of the protein. This catalytic domain, consisting of eight  $\alpha$ -helices and a single five-stranded  $\beta$ -sheet, is centrally located within the protein structure and forms an interface with each of the three other domains.<sup>77</sup> *PfA*-M1 contains a single catalytic Zn(II) ion within the active site, a feature which is conserved across the M1-family of aminopeptidases.<sup>67,78</sup> Other notable structural characteristics of the M1 aminopeptidase family are two conserved sequence motifs that contribute to the active site: a HEXXHX18E zinc-binding motif, and the GXMEN substrate recognition motif.<sup>67,68,79</sup> Indeed, the presence of both a H496EYFHX<sub>17</sub>KE519 and a G460AMEN active site motif in *PfA*-M1 has been noted, as highlighted in Table 3.<sup>68,70,73,74</sup> The single catalytic Zn(II) ion is coordinated by His496, His500, Glu519 and a nucleophilic water molecule in the native, ligand-free form of the enzyme. This water molecule, which is also coordinated by Glu463 and Glu497, forms a longer metallo-bond with the Zn(II) ion. A two-step catalytic mechanism has been proposed, whereby molecular dynamic simulations were used to predict the formation of two conformationally-distinct transition states.<sup>77</sup> The formation of the second transition state involves rotation of Glu497 in order for hydrolysis to occur.

The active site cavity itself is buried within the catalytic domain and can be accessed *via* two connecting apertures: the N-terminal opening and the C-terminal opening. The N-terminal opening can be found at the junction of domains I and IV, and offers a small groove of only 8 Å. The C-

terminal opening is larger and is formed by the cone-shaped superhelical structure of domain IV giving rise to a channel leading to the active site that is approximately 30 Å in length and 13 Å in diameter.

The active site structure allows for a range of hydrophobic and basic N-terminal residues to be cleaved by *PfA-M1*

Despite being also termed an alanyl aminopeptidase, *PfA-M1* displays a broad preference towards a variety of residues at the N-terminal P<sub>1</sub> position, but particularly those that are hydrophobic or basic. In fact, the amino acids most preferentially cleaved from Xaa-7-amino-4-carbamoylmethylcoumarin (ACC) substrates by this enzyme were found to be Met and Leu. Ala, Arg, Lys, Phe, Tyr and Trp are also cleaved, albeit with decreasing efficiency.<sup>70,80,81</sup> In addition, a library of unnatural amino acids coupled to ACC was also tested as substrates for *PfA-M1*, and it was found that some of these were hydrolyzed more efficiently than the natural amino acid-ACC fluorogenic substrates.<sup>80</sup>

Catalytic activity is also influenced by substrate interaction at the S<sub>1</sub>' sub-site of *PfA-M1*.<sup>81</sup> The kinetic parameters ( $K_m$  and  $k_{cat}$ ) were altered favourably to increase catalytic activity when basic and hydrophobic residues were present at P<sub>1</sub>'. This observation is consistent with those seen for other M1 aminopeptidases.<sup>76,82-84</sup>

*PfA-M1* localizes to multiple compartments within the parasite

The subcellular localization of *PfA-M1* has been widely debated, although it is now accepted that *PfA-M1* localizes to several compartments within the parasite. *PfA-M1* is found in the cytosol, the FV and the nucleus.<sup>36,39,69</sup> How *PfA-M1* is trafficked to the nucleus and its role here is still unclear, however, it is thought that the signal for nuclear localization is not contained within the NTE.<sup>36</sup>

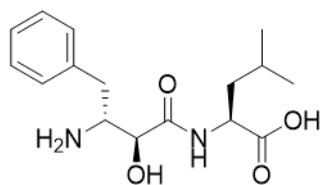
### *pH stability*

Since *PfA-M1* is localized within both the cytosol and the FV, the effect of pH on enzyme stability and catalytic efficiency is important. The pH of the digestive FV of *Pf* has been estimated at between pH 5.0 – 5.5, whereas the cytosol is neutral.<sup>85–87</sup> The contrast in pH between the two environments means that the enzyme must be able to function efficiently across a wide range of pH values. As expected, when tested for stability across the pH range 5.0 – 8.5, it was found that *PfA-M1* stability was largely undisturbed with  $\geq 90\%$  of the starting activity remaining after 1 hour at all pH values tested.<sup>69</sup> This data is consistent with a functional *PfA-M1* in both the neutral and acidic environments of the cytosol and FV, respectively.

### Development of inhibitors towards *PfA-M1*

A number of inhibitors based on a variety of structurally distinct chemical scaffolds have been identified, including bestatin-based analogues<sup>38,88</sup>, phosphinate dipeptide analogues<sup>70,89</sup> and hydroxamic acid-containing compounds<sup>90,91</sup>. There is only 26% sequence similarity between *PfA-M1* and hAPN, the human M1 ortholog with the highest sequence identity to *PfA-M1*, giving rise to the prospect of developing parasite-selective inhibitors of *PfA-M1*.<sup>38,88</sup>

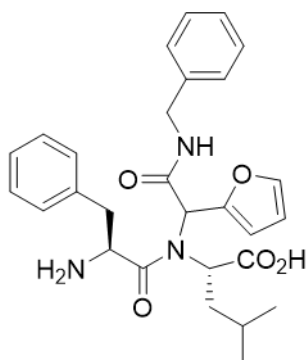
(-)-Bestatin (**5**, Figure 5) is a naturally derived dipeptide analogue of Phe-Leu obtained from the bacterium *Streptomyces olivoreticuli*.<sup>38,88,92,93</sup> It is a reversible inhibitor of a number of MAPs, and is an effective inhibitor of r*PfA-M1* ( $K_i$ , 478 nM).<sup>70</sup> Importantly, bestatin inhibits both *in vitro* and *in vivo* growth of *Pf*.<sup>35,94</sup> However, bestatin has drawbacks which limit its use as an effective drug molecule. It is an inhibitor of a number of MAPs across species and so selectivity towards the parasite could not be achieved. Furthermore, the dipeptide structure of bestatin is predicted to generate an unfavourable PK profile, meaning the ability of the drug to reach the site of action would be compromised.



5  
Bestatin

**Figure 5:** Bestatin, a reversible broad-range MAP inhibitor.<sup>93</sup>

Utilization of a combinatorial multicomponent Ugi reaction to produce a library of peptidomimetic compounds identified a bestatin-derived peptidomimetic, KBE009 (**6**, Figure 6), that inhibited *PfA*-M1 with a  $K_i$  of 400 nM.<sup>95</sup> In this case, **6** was obtained, and subsequently used in the biological screening process, as a mixture of diastereomers. KBE009 and bestatin were also equipotent at inhibiting growth of *in vitro* cultures of *Pf* (3D7 strain) (bestatin  $IC_{50}$ ,  $21 \pm 4 \mu\text{M}$ ; KBE009  $IC_{50}$ ,  $18 \pm 7 \mu\text{M}$ ).<sup>95</sup> Interestingly, KBE009 displayed a >250-fold selectivity towards the malarial enzyme over a mammalian ortholog, pig APN.<sup>95</sup> KBE009 may offer an advantage over bestatin because the tertiary amide bond is predicted to slow down, or provide resistance to, proteolysis and improved PK parameters compared to bestatin, whilst retaining anti-malarial activity.<sup>96</sup>



6  
KBE009

**Figure 6:** KBE009.<sup>95</sup>

CQ (**7**, Figure 7) exerts its antimalarial activity through inhibition of the heme detoxification pathway, leading to build-up of toxic heme which is lethal to the parasite.<sup>10,11,97</sup> It was widely considered the preferred antimalarial treatment after its discovery in the 1930s, however rapid emergence of resistance in the 1960s led to it being replaced or used in combination with other medications.<sup>13,14</sup>

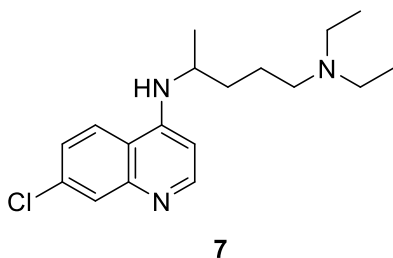


**Figure 7:** Chloroquine.<sup>11</sup>

Now, CQ is rarely used for the treatment of *Pf* malaria due to widespread resistance. Nonetheless, a series of quinoline-based inhibitors aimed at dual inhibition of the heme detoxification pathway and *PfA*-M1 have been developed.<sup>91</sup> An in-house screen of quinoline-based compounds identified hit compound **8** (Figure 8), from which a library of 45 non-peptidic analogues were synthesized providing three hit compounds (**9**, **10** and **11**, Figure 8) as inhibitors of native *PfA*-M1, with IC<sub>50</sub> values of 0.85 to 2.50  $\mu$ M (Table 4).<sup>91</sup> The hydroxamic acid metal-chelating group was crucial for activity since the carboxylic acid analogues of **9** and **10** were found to be inactive. The isobutyl group was also found to be essential as removing this group led to inactive analogues. Compounds **9**, **10** and **11** were then tested for their ability to inhibit parasite growth *in vitro* against the CQ-resistant strain (FcB1) and for selectivity over the mammalian APN.<sup>91</sup> All three compounds displayed sub-micromolar inhibition of parasite growth (0.15 to 0.32  $\mu$ M), however they were also found to be inhibitors of the mammalian APN.<sup>91</sup> To conclude, the quinoline and hydroxamic acid moieties allows these compounds to demonstrate antimalarial

activity through dual inhibition of heme detoxification and *PfA*-M1. Activity against *PfA*-M1 and issues surrounding selectivity need to be addressed before these compounds can be progressed further.

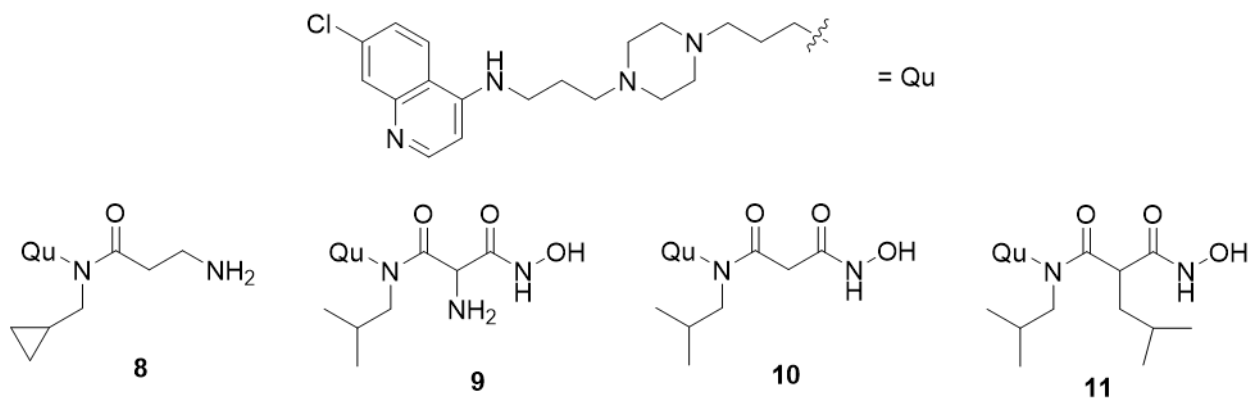


**Figure 8:** Structures of the quinoline-based inhibitors.<sup>91</sup>

**Table 4:** Inhibition of native *PfA*-M1, effect on proliferation of *Pf* FcB1 *in vitro* and selectivity against mammalian pig APN by the quinoline-based inhibitors.<sup>91</sup>

Compound	IC <sub>50</sub> <i>PfA</i> -M1 (μM)	IC <sub>50</sub> <i>in cellulo</i> (FcB1) (μM)	IC <sub>50</sub> <i>in vitro</i> (mammalian APN) (μM)
<b>8</b>	21	0.398 ± 0.056	28
<b>9</b>	2.503	0.178 ± 0.037	1.345
<b>10</b>	0.854	0.317 ± 0.063	0.028
<b>11</b>	1.540	0.151 ± 0.013	1.628

A new series of MAP inhibitors, the phosphinate dipeptide analogues, was identified and yielded a hit which displayed more potent inhibition of *rPfA*-M1 than bestatin.<sup>89</sup> hPheP[CH<sub>2</sub>]Phe (**12**, Figure 9), also termed Co4, achieved potent inhibition of *rPfA*-M1 with a *K<sub>i</sub>* value of 79 nM.<sup>70</sup> In addition, when administered at a dose of 100 mg/kg twice daily, Co4 showed a high level of antimalarial activity in the murine *P. c. chabaudi* model, reducing levels of infection by 92%

whereas bestatin was only able to reduce the levels of infection by 34% in the equivalent model.<sup>98</sup> Co4 is also a potent inhibitor of the *rPfA*-M17 aminopeptidase and therefore part of the Co4 antimalarial activity might result from inhibition of this second enzyme. A second analogue, hPheP[CH<sub>2</sub>]Tyr (**13**, Co5) is also a potent *rPfA*-M1 inhibitor ( $K_i$ , 232 nM), albeit with a higher  $K_i$  compared to Co4.<sup>98</sup>

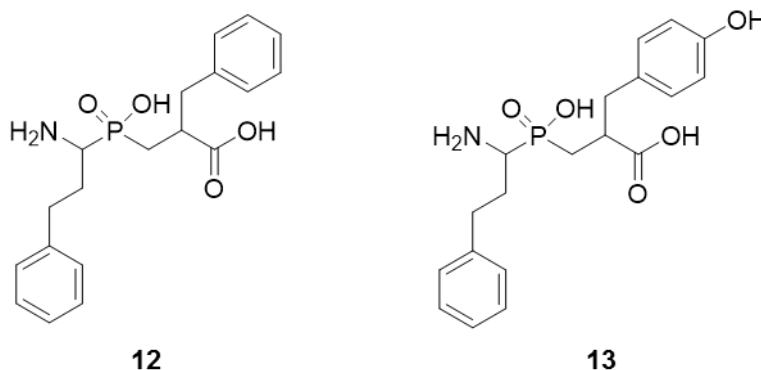


**Figure 9:** The most potent phosphinate dipeptide inhibitors capable of inhibiting *rPfA*-M1.<sup>89,98</sup> In these studies, Co4 (**12**) and Co5 (**13**) were used as mixtures of four diastereomers.

In the studies looking at Co4 and Co5, it is notable that the inhibitors were used as mixtures of four diastereomers. Since the most active stereoisomer of bestatin is (2*S*,3*R*)-AHPA-(*R*)-Leu, it has been proposed that the (*R*)-hPheP[CH<sub>2</sub>]-(*R*)-Phe (Co4) and (*R*)-hPheP[CH<sub>2</sub>]-(*R*)-Tyr (Co5) stereoisomers are the most active of the four.<sup>98</sup>

PK differences between these organophosphorus inhibitors and bestatin have been proposed as the reason for the large increase in *in vivo* antimalarial activity of the former. Bestatin is taken up into the RBCs very slowly and is rapidly cleared from serum. Whilst the corresponding properties of Co4 are unknown, the greater hydrophobicity of the phosphinate dipeptide compound is expected to confer greater target accessibility and persistence in the body compared to bestatin, which might explain the more potent antimalarial effect observed.

A potent and highly selective amino-benzosuberone derivative, T5 (**14**, Figure 10), also displays promising *in vitro* and *in vivo* activity.<sup>99–101</sup> A racemic mixture of T5 selectively inhibited *PfA*-M1 with a  $K_i$  value of 50 nM, with no inhibitory action against *PfA*-M17 ( $K_i > 100 \mu\text{M}$ ). In addition, T5 added to *in vitro* cultures of CQ-resistant (FcB1) and a CQ-sensitive (3D7) *Pf* strain gave good levels of growth inhibition with similar  $\text{IC}_{50}$  values of  $6.5 \pm 2.4 \mu\text{M}$  (FcB1) and  $11.2 \pm 3.4 \mu\text{M}$  (3D7).<sup>99</sup> T5 was also effective in reducing parasitaemia at the peak of infection in the murine model, *P. c. chabaudi*. Doses of 12 and 24 mg/kg led to a reduction in parasitaemia at the peak of infection by 40–44%, a result deemed to be of statistical significance.<sup>99</sup> This study suggests that T5 may provide a novel scaffold for the future development of potent, selective inhibitors against *PfA*-M1.

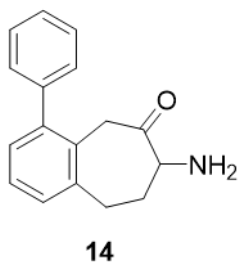


**Figure 10:** The racemic, selective *PfA*-M1 inhibitor, T5.<sup>99–101</sup>

The recent release of the X-ray crystal structure of *PfA*-M1 in complex with T5 (PDB ID: 6SBQ) has provided an insight into the binding mode of the inhibitor (Figure 11).<sup>72</sup> The seven-membered ring adopts a chair-like conformation and the ketone functionality is present as the hydrated, diol form. One hydroxyl group is able to coordinate the Zn(II) ion along with forming a hydrogen bond with Tyr580, and the second hydroxyl group forms a hydrogen bond with Glu497. The primary amine forms three hydrogen bond interactions with Glu319, Glu463 and Glu519. The phenyl ring is situated in the  $S_1'$  pocket and forms  $\pi$ - $\pi$  stacking interactions with the imidazole side chain of His496.

Analysis of the binding site identified key interactions, particularly in the S<sub>1</sub>' pocket where the phenyl ring lies, which could be exploited to increase binding affinity. Addition of chemical moieties to the phenyl ring to extend T5 into this pocket may enable further interactions, for example with Glu526 which points into the active site.<sup>72</sup> This information may be employed to drive the synthesis of future T5 analogues.

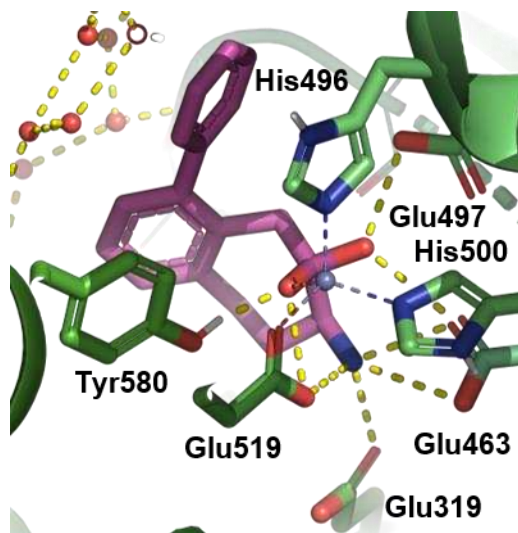


**Figure 11:** Binding pose of T5 (pink, **14**, present as the hydrated, diol form) in the active site cavity of *PfA-M1* (PDB ID: 6SBQ).<sup>72</sup> The catalytic Zn(II) ion is shown as a blue sphere; water atoms are shown as red spheres. All molecules are colored according to atom. Interactions with the metal ion are shown as blue dashed lines, polar interactions are shown as yellow dashed lines. Image generated using PyMOL.<sup>102</sup>

Unfortunately, T5 demonstrated high clearance (43 mL/min/kg) and a relatively short half-life ( $T_{1/2}$ ) of 2.2 hours following intravenous dosing to female CD-1 mice.<sup>72</sup> The high level of clearance from mice, coupled with solubility issues, represent key areas to focus on for the further development of aminobenzosuberone derivatives.

A series of malonic hydroxamates have also been identified as potent inhibitors of native, purified *PfA*-M1 and have been subjected to optimization through the introduction of steric constraints.<sup>90</sup> One of these hydroxamates, BDM14471 (**15**, Figure 12), demonstrated potent *rPfA*-M1 inhibition ( $K_i$ , 6 nM), and >200-fold selectivity for the malarial enzyme when tested against pig APN.<sup>90</sup> Additionally, BDM14471 was tested against both CQ-resistant (FcB1) and CQ-sensitive (F32) strains, inhibiting parasite growth by 24  $\mu$ M and 13  $\mu$ M, respectively.<sup>90,103</sup> Although BDM14471 was able to reach the site of action in the RBCs, the observed *in vitro* potency was weak and disappointing considering how potent this compound was at inhibiting the enzyme. PK experiments found that BDM14471 was stable in both rat plasma ( $t_{1/2}$  = 22 hours) and human plasma ( $t_{1/2}$  > 24 hours).<sup>90,103</sup> *In vivo* experiments using female CD1 mice dosed at 50 mg/kg intraperitoneally indicated BDM14471 accumulation within the RBCs and, hence, the discrepancy observed between the strength of enzymatic inhibition and antiparasmodial activity is unlikely to be due to molecular properties preventing it from reaching the site of action.<sup>103</sup>

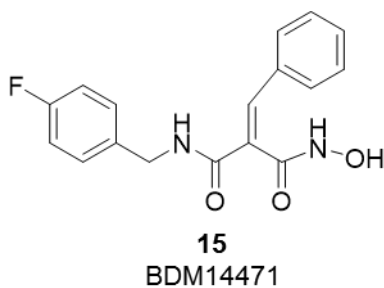


**Figure 12:** Malonic hydroxamate, BDM14471.<sup>90</sup>

Leucyl aminopeptidase

*PfA-M17*, a 67.8 kDa protein belonging to the M17 family of metalloproteases. Similar to *PfA-M1*, *PfA-M17* is specific for the cleavage of hydrophobic N-terminal residues from peptide substrates.

*PfA-M17* adopts the conserved hexameric structure

*X-ray crystal structure*

A truncated form of *PfA-M17* (*rPfA-M17*, residues 83-598) was expressed and characterized, and subsequently shown to be functionally active.<sup>104</sup> The X-ray crystal structures of *rPfA-M17* at 2Å with either a single Zn(II) ion (PDB ID: 3KQX) or two Zn(II) ions (PDB ID: 3KQZ) bound at the active site have been solved.<sup>105</sup> The structure comprised two hexamers in the asymmetric unit, which is similar to the structures adopted by other members of the M17 family.<sup>106,107</sup> Each monomer consists of an N-terminal domain (residues 85-276) and a C-terminal catalytic domain (residues 301-605), linked together through a ~30 Å helix (residues 277-300) which runs through the centre of the monomer, as illustrated in Figure 13.

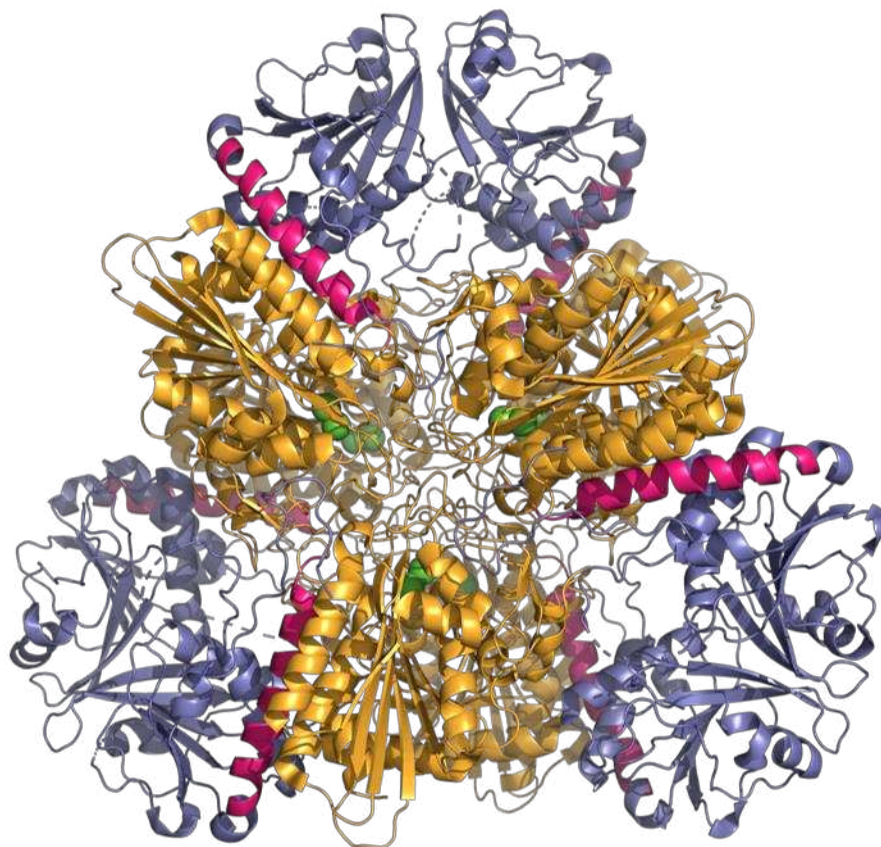


**Figure 13:** The X-ray crystal structure of *PfA-M17* (PDB ID: 3KQZ).<sup>105</sup> Each *PfA-M17* monomer is colored by domain: the N-terminal domain (residues 83-276) is shown in blue, linker residues 277-300 are colored pink and the C-terminal catalytic domain (residues 301-605) is shown in orange. The catalytic metal ions are shown as green spheres. Image generated using PyMOL.<sup>102</sup>

Within the asymmetric unit, the monomers align themselves so as to position the six active sites towards the interior of the complex, forming a central disk-like cavity measuring  $\sim 35$  Å in diameter and  $\sim 15$  Å in height. This enclosed active site cavity is accessed through channels in the monomer N-terminal domains. Partially disordered loops ( $\sim 20$  Å) found in 10 of the 12 monomers appear to guard the entrance to the active site cavity and are likely to function in regulating substrate access.<sup>105</sup>

### *Active site*

The C-terminal domain of the *PfA-M17* monomer is made up of a central  $\beta$ -sheet which is bordered on either side by nine  $\alpha$ -helices and has a two stranded  $\beta$ -sheet capping one end. The active site cavity positioned close to the edge of the central  $\beta$ -sheet measures 18 Å by 18 Å and is dominated by negatively charged residues that in the di-zinc structure coordinate with the two catalytic metal ions positioned 2.9 Å apart.<sup>105</sup> The site 1 Zn(II) ion is coordinated by residues Asp379, Asp459, and Glu461, whereas coordination of the site 2 Zn(II) ion involves Lys374, Asp379, Asp399, Glu461 and two water molecules.<sup>104,105</sup>

### *Metal-ion content*

A defining characteristic of leucyl aminopeptidases (LAPs) is the presence of two metal binding sites within the active site.<sup>107</sup> Binding affinities of these two sites have been studied across species and have been found to be inequivalent. Site 1 is readily exchangeable and so is termed a loose-binding site, whereas site 2 binds Zn<sup>2+</sup> tightly and is called the catalytic site.<sup>108–110</sup>

*PfA-M17* is highly specific for the cleavage of hydrophobic N-terminal residues

In comparison to *PfA-M1*, *PfA-M17* displays a much narrower specificity for P<sub>1</sub> residues, although the two aminopeptidases do show some overlap in the substrates they favour. *PfA-M17* exhibits a strong preference for N-terminal hydrophobic residues, in particular Leu and Trp, which is consistent with the crystal structure that shows that the S<sub>1</sub> subsite of the enzyme is lined by hydrophobic residues Met392, Met396, Phe398, Gly489, Leu492, and Phe583.<sup>80,104,105</sup> The highly hydrophobic nature of the active site explains the specificity for peptides with hydrophobic N-terminal residues, especially Leu, and the inability of the enzyme to cleave polar amino acids from peptides substrates.<sup>80</sup> The lack of *PfA-M17* activity towards substrates with small N-terminal amino acids (e.g. Ala and Gly) can be attributed to the fact that these residues do not extend far enough into the S<sub>1</sub> subsite to form interactions which promote substrate binding.<sup>105</sup>

This narrow substrate specificity of *PfA-M17* and strong preference for Leu at P<sub>1</sub> is of note since it is not a conserved feature of LAPs across species.<sup>106,111</sup> The physiological reason for this specificity is not fully understood but it has been proposed that the main function of *PfA-M17* is to generate free Leu from host Hb. Ile is one of the most abundant amino acids in *Pf* proteins and thus vital for parasite growth and cell maintenance. However, Ile is absent from Hb and must be sourced from outside of the RBC *via* channels that import the amino acid in exchange for Leu.<sup>112</sup> Hence, the narrow substrate specificity of *PfA-M17* is thought to have evolved to play a key role in catabolism of peptides to generate high concentrations of intracellular Leu to then exchange for vital Ile.<sup>43,80,104,113</sup>

*PfA-M17* localizes to the parasite cytosol

*PfA-M17* resides in the cytosol of the parasite as revealed by immunohistochemistry using antiserum raised to recombinant enzyme and by using parasites expressing *PfA-M17* tagged with either green or yellow fluorescent protein (YFP).<sup>23,36</sup>

Development of inhibitors towards *PfA-M17*

As with *PfA-M1*, *PfA-M17* is inhibited by bestatin, Co4 (**12**) and Co5 (**13**) with all three compounds displaying greater potency towards the leucyl aminopeptidase than against the alanyl aminopeptidase (bestatin  $K_i = 25$  nM, compared to 478 nM; Co4  $K_i = 13$  nM compared to 79 nM; Co5  $K_i = 10$  nM compared to 232 nM).<sup>98,104,105</sup> X-ray crystal structures of *PfA-M17* in complex with both bestatin (*PfA-M17*-BES, PDB ID: 3KR4) and Co4 (*PfA-M17*-Co4, PDB ID: 3KR5) revealed that the inhibitors interact with the active site of the enzyme in a similar manner, albeit forming slightly different coordination interactions with the catalytic metal ions (Figure 14).<sup>105</sup> Molecular docking studies predict the hydroxyl group of the P<sub>1</sub> Tyr residue in Co5 to be solvent exposed and not involved in any hydrogen bonding interactions, which is consistent with the very similar  $K_i$  values reported for **12** and **13**.<sup>105</sup> Comparison with the corresponding enzyme/inhibitor

crystal structures obtained from *PfA*-M1 also identified more extensive interactions for each inhibitor with the active site residues of *PfA*-M17 compared to *PfA*-M1, hence increasing the binding affinity in the former.<sup>105</sup>

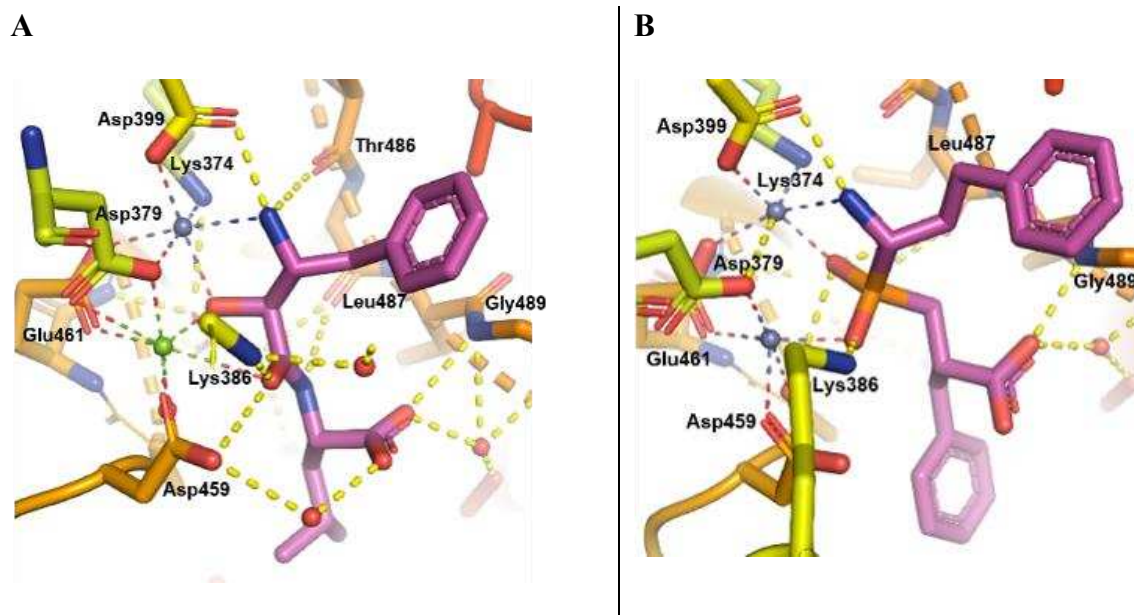


**Figure 14:** Binding poses of A) bestatin (**5**, PDB ID: 3KR4), and B) Co4 (**12**, PDB ID: 3KR5) to *PfA*-M17.<sup>105</sup> Inhibitor molecules are shown in purple and all molecules are colored according to atom. Water molecules are shown as red spheres; Zn(II) ions as blue spheres; Mg(II) ions as green spheres. Polar interactions are indicated by yellow dashed lines; interactions with the metal ions are indicated by multi-colored dashed lines. Images generated using PyMOL.<sup>102</sup>

Bestatin and two derivatives, nitrobestatin (**16**) and bestatin methyl ester (**17**) (Figure 15), inhibit both *rPfA*-M17 activity and *in vitro Pf* growth (strain DC10).<sup>104</sup> Although nitrobestatin ( $K_i$ , 2.7 nM) is 10-fold more potent against *rPfA*-M17 than bestatin ( $K_i$ , 25 nM), its ability to inhibit *in vitro* parasite growth was only improved by around 2-fold ( $IC_{50}$ , 8  $\mu$ M compared to 14.87  $\mu$ M).<sup>104</sup> Bestatin methyl ester displayed lower inhibitory activity against both *rPfA*-M17 ( $K_i$ , 138 nM) and *in vitro* parasite growth ( $IC_{50}$ , 20.5  $\mu$ M), when compared to bestatin.<sup>104</sup>

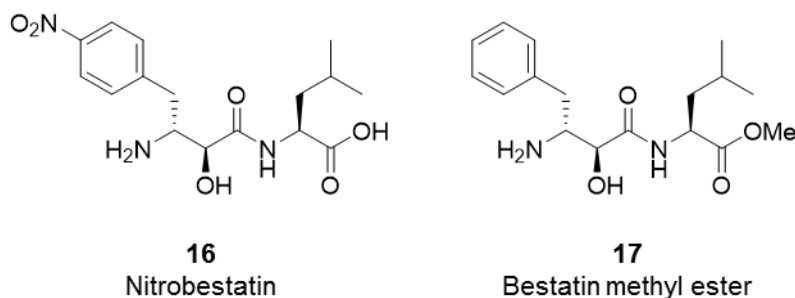


**Figure 15:** Bestatin analogues capable of inhibiting *rPfA*-M17.<sup>104</sup>

Bestatin and the analogues **16** and **17** are highly polar, which is expected to slow the rate of uptake into the erythrocytes due to poor cell membrane permeability. However, the reduced polarity of **17** compared to **5** may explain why **17** is >5-fold less potent against the free enzyme than **5**, but demonstrates a similar potency for inhibiting parasite growth as increased cell permeability allows for higher concentration of **17** to reach the site of action.

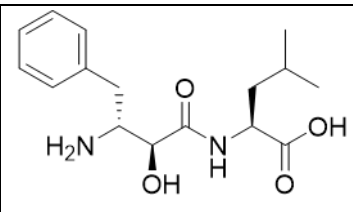
#### Dual inhibitors of *PfA*-M1 and *PfA*-M17

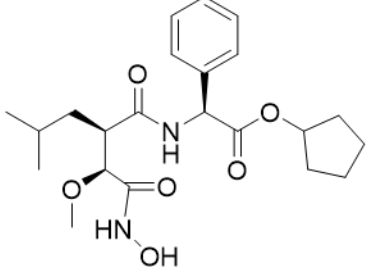
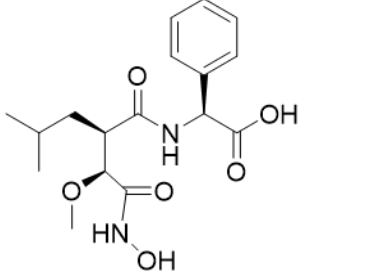
Within the *Pf* genome, *PfA*-M1 and *PfA*-M17 are often studied together since, collectively, these two enzymes are responsible for the release of all neutral amino acid residues found in soluble *Pf* cytosolic extracts.<sup>23,70,104</sup> The two enzymes have historically been referred to as the “neutral aminopeptidases” however this term is no longer accurate since *PfA*-M1 has been shown to also cleave basic N-terminal residues.

A drug repurposing study found that a hydroxamate-derivative of the chemotherapeutic drug Tosedostat is a potent inhibitor of both *PfA*-M1 and *PfA*-M17 and is orally active against murine malaria.<sup>114,115</sup> This hydroxamate-containing ester, CHR-2863 (**18**, Table 5), is converted into the acid-derivate, CHR-6768 (**19**), *in situ* through hydrolysis by esterase enzymes. CHR-2863 and CHR-6768 inhibit *rPfA*-M1 with a similar potency ( $K_i$ , 1.4  $\mu$ M and 2.4  $\mu$ M, respectively) to that of bestatin ( $K_i$ , 1.6  $\mu$ M).<sup>114</sup> Both inhibitors display higher potency against *rPfA*-M17 (CHR-2863,

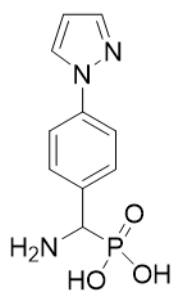
$K_i$ , 75 nM and CHR-6768,  $K_i$ , 25 nM) which is respectively 8- and 24-fold greater than bestatin.<sup>114</sup> CHR-2863 (IC<sub>50</sub>, 370 nM) is a more potent inhibitor of parasite growth compared to bestatin (IC<sub>50</sub>, 5 μM) in an *in vitro* culture of the *Pf* strain 3D7 and was 5-fold more potent than the acid form, CHR-6768 (IC<sub>50</sub>, 2 μM).<sup>114</sup> The improved antimalarial efficacy of the ester probably reflects the increased hydrophobicity and expected membrane permeability of the compound. A similar *in vitro* antimalarial potency for CHR-2863 was also seen against the *Pf* multidrug-resistant strain, K1.<sup>114</sup> Importantly, CHR-2863 was able to significantly reduce the peak parasitaemia in a *P. c. chabaudi* murine model of infection.<sup>114</sup> This result is also significant in that the mice were dosed orally, providing evidence that CHR-2863 is orally bioavailable.

**Table 5:** Summary of the inhibitory parameters shown by the hydroxamate-containing inhibitors, CHR-2863 (**18**) and CHR-6768 (**19**), in comparison with the natural product inhibitor, bestatin (**5**). IC<sub>50</sub> values *in vitro* were determined through the prevention of [<sup>3</sup>H]hypoxanthine incorporation. *P. c. chabaudi* *in vivo* activity was measured using a modified 4-day suppression test.<sup>114</sup> N.D = Not determined.

Compound	$K_i$ rPfA-M1 (nM)	$K_i$ rPfA-M17 (nM)	IC <sub>50</sub> <i>in vitro</i> (μM) ( <i>Pf</i> strain)	<i>In vivo</i> parasitaemia reduction ( <i>P. c. chabaudi</i> ) (Dosage per day for 4 days)
<b>5</b> 	1673 ± 238.05	613 ± 201.33	5 (3D7)	34% (100 mg/kg)

18		1413.41 ± 123.74	75.96 ±22.86	0.37 (3D7)  0.376 (K1)	43% (25 mg/kg) 52% (50 mg/kg) 66% (100-50 mg/kg)
19		2409.62 ± 316.02	25.71 ± 7.89	2 (3D7)	N.D

An aminophosphonate compound, **20** (prepared as a racemic mixture, Figure 16), is also described by the authors as showing dual inhibition of *PfA*-M1 and *PfA*-M17, but in this instance by coordinating the active site metal ions through the phosphonate group.<sup>116</sup> However, whilst **20** exhibits potent inhibition of r*PfA*-M17, inhibition of r*PfA*-M1 is very weak and so may not be truly considered a dual inhibitor of these enzymes (r*PfA*-M1  $K_i$ , 104  $\mu$ M; r*PfA*-M17  $K_i$ , 11 nM).<sup>116</sup> Additionally, the phosphonic acid would exist as a dianion at physiological pH which might limit membrane permeability of **20**.



**20**

**Figure 16:** The most potent aminophosphonate reported to be capable of inhibiting both *PfA*-M1 and *PfA*-M17.<sup>116</sup>



discovery of compound 10o (**23**, Figure 18) as one of the most potent dual inhibitors of *PfA-M1* and *PfA-M17* described to date (*rPfA-M1*  $K_i$ , 76 nM, *rPfA-M17*  $K_i$ , 60 nM).<sup>118,119</sup> Most notably, **23** also displayed potent, nanomolar inhibition of *in vitro* parasite growth against strains 3D7 (CQ-sensitive,  $IC_{50}$ , 126 nM), Dd2 (CQ-, quinine-, pyrimethamine- and sulfadoxine-resistant,  $IC_{50}$  = 189 nM) and also NITD609-RDd2 clone#2 (resistant to the same parent drugs as Dd2, but additionally resistant to spiroindolones, aminopyrazoles, dihydroisoquinolones and pyrazolamindes,  $IC_{50}$ , 107 nM).<sup>118</sup> Furthermore, **23** displayed no toxicity towards HEK293 cells up to a concentration of 40  $\mu$ M and PK studies found that the solubility and metabolic stability of the inhibitor were promising.<sup>118</sup> Co-crystallisation of a racemic mixture of 10o with both *PfA-M1* and *PfA-M17* revealed that the *R*-enantiomer was preferentially bound in the crystal structure of the enzyme-inhibitor complexes, suggesting that this is the most active enantiomer.<sup>118</sup>

The potent inhibition of both *PfA-M1* and *PfA-M17* by **23** was partially attributed to the 3,4,5-trifluorophenyl moiety.<sup>118</sup> The X-ray crystallographic data showed that in *PfA-M1* the fluorine atoms are able to form a water-mediated hydrogen bonding network, whilst in the *PfA-M17* active site the trifluorophenyl ring forms hydrophobic interactions with residues Met392, Leu492 and Phe583.<sup>53,118</sup> Importantly, **23** was equally potent towards both *PfA-M17* and *PfA-M1*, which is clearly advantageous over single-enzyme inhibitors. Dual inhibition of both aminopeptidases may slow the development of parasite resistance to this class of antimalarial drugs and prolong their antiparasitic usefulness in the field.

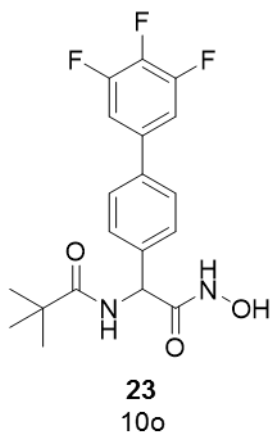


**Figure 18:** 10o.<sup>118</sup>

In a further study aimed at optimizing interactions made with the  $S_1'$  subsite of both enzymes, a series of compounds based on **10o** were synthesized in which modifications were made to the N-pivaloyl group.<sup>53</sup> Using a modified Morrison equation to measure  $K_i$  values, **23** exhibited slightly higher binding affinities in this study (*rPfA*-M1  $K_i$ , 331 nM, *rPfA*-M17  $K_i$ , 147 nM) than previously reported.<sup>118,119</sup> Of the compounds synthesized, **24** (Figure 19) was found to be the most potent *PfA*-M1 inhibitor (*rPfA*-M1  $K_i$ , 88.9 nM) whilst **25** (Figure 19) displayed potent inhibition of *PfA*-M17 (*rPfA*-M17  $K_i$ , 101 nM).<sup>53</sup> Crucially, both **24** and **25** were able to demonstrate improved anti-parasitic activity (**24** *Pf*-3D7  $IC_{50}$ , 76.8 nM, *Pf*-Dd2  $IC_{50}$ , 24.1 nM; **25** *Pf*-3D7  $IC_{50}$ , 14.6 nM, *Pf*-Dd2  $IC_{50}$ , 13.8 nM) in comparison to **23** (*Pf*-3D7  $IC_{50}$ , 83.1 nM, *Pf*-Dd2  $IC_{50}$ , 81.7 nM).<sup>53</sup> Additionally, only minor inhibition of HEK293 cell proliferation was observed at 10  $\mu$ M for both **24** and **25**, suggesting limited cytotoxicity of these compounds.<sup>53</sup> To further investigate off-target toxicity effects, **25** was tested for its ability to inhibit a panel of five matrix metalloproteinases (MMPs) and two human aminopeptidases, hAPN and insulin-regulated aminopeptidase (IRAP). **25** showed no, or very weak levels of, inhibition against the MMPs and IRAP, however it was shown to be a moderate inhibitor of hAPN ( $K_i = 0.3 \mu$ M).<sup>53</sup> With this in mind, **25** can be considered a promising lead compound for the development of future antimalarial therapies.

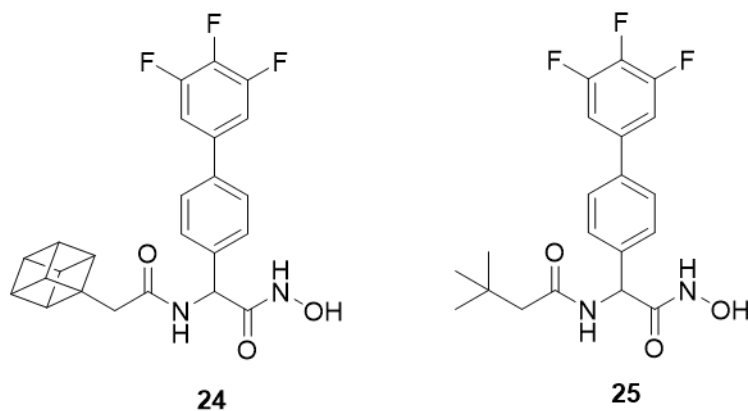


**Figure 19:** Structures of the potent *PfA*-M1 and *PfA*-M17 inhibitors.<sup>53</sup>

### Cross species inhibition of *Pf* and *Pv*

An important consideration in the development of novel antimalarial therapies is the potential for cross-species inhibition. Similar to dual inhibition of enzymes within *Pf*, cross-species inhibition would be advantageous to increase effectiveness of new therapies. In addition to *Pf* parasites, homologous M1 and M17 enzymes are also present in *Pv* (*Pv*-M1 and *Pv*-M17) and so a recent study looked at the potential for cross-species inhibition.<sup>53</sup> A high degree of active site sequence homology between the species has been noted: *PfA*-M1 and *Pv*-M1 share 89% catalytic domain sequence homology, whilst *PfA*-M17 and *Pv*-M17 share 92% sequence homology in the catalytic domain, which reduces the challenge of inhibitor development against all four enzymes.<sup>53</sup> Indeed, this study found that a series of inhibitors followed the same trend in potency against both *PfA*-M1 and *Pv*-M1, albeit inhibition of *Pv*-M1 was approximately 10-fold greater across the series. Inhibition of *PfA*-M17 and *Pv*-M17 also largely followed the same trend across the series but, in comparison to the M1 enzymes, the scale of inhibition was largely conserved for each inhibitor.<sup>53</sup> The most promising inhibitors identified in this series, **24** and **25** (Figure 19), were able to potently inhibit both *Pv*M1 and *Pv*-M17 (**24** *rPv*-M1  $K_i$ , 1.73 nM, *rPv*-M17  $K_i$ , 77.9 nM ;**25** *rPv*-

M1  $K_i$ , 6.39 nM, rPv-M17  $K_i$ , 3.60 nM).<sup>53</sup> As a result, this series of compounds represents a promising step forward in the design of novel antimalarial therapeutics which not only have the ability to target multiple enzymes within a single *Plasmodium* species, but also to provide cross-species inhibition.

### Aspartyl aminopeptidase

*Pf*M18AAP, an aspartyl aminopeptidase belonging to the M18 family of metalloproteases, is a ~65 kDa cytoplasmic protein possessing two zinc ions in the catalytic site.<sup>67</sup> Although classed as an aspartyl aminopeptidase, the specificity of the *Pf* enzyme extends to glutaminy substrates.<sup>120,121</sup> Gene knockouts of *Pf*M18AAP have resulted in viable parasites, suggesting the enzyme is not essential for parasite growth, however a fitness cost to the parasite was observed.<sup>36</sup> Antisense-induced knockdown of *Pf*M18AAP expression resulted in lethality accompanied by abnormal FV morphology in ring and schizont stages and the appearance of large lipid droplets and accumulation of Hb in trophozoites.<sup>122</sup>

The 3D structure of *Pf*M18AAP contains the conserved M18 aminopeptidase fold

#### *X-ray crystal structure*

The X-ray crystal structure of *Pf*M18AAP was solved to 2.6 Å (PDB ID: 4EME)<sup>120</sup>, in which the complete unit cell of *Pf*M18AAP was found to be made up of 12 monomers arranged in a dodecameric assembly. The *Pf*M18AAP monomer comprises two domains: a catalytic domain (residues 1-91 and 307-577), and a regulatory domain (residues 92-306). The tertiary structure of these domains is arranged to form the characteristic M18 aminopeptidase fold.<sup>121</sup> The catalytic domain is made up of ten  $\alpha$ -helices which line a central seven-stranded  $\beta$ -sheet; this  $\alpha\beta$  arrangement is also topped by an additional four-stranded antiparallel  $\beta$ -sheet. The top of the catalytic domain is largely made up of unstructured loop regions which, in conjunction with the

central  $\beta$ -sheet, form the active site of the monomer. The regulatory domain is made up of two three-stranded antiparallel  $\beta$ -sheets around a helix formed by residues 279-289, along with a second helix and an expansive loop region. High levels of disorder along with breaks in electron density for residues 163-169 and 197-272 indicate the large degree of flexibility within the regulatory domain.

The 3D arrangement of *PfM18AAP* adopts a tetrahedral geometry made up of both a dimeric and a trimeric interaction.<sup>120</sup> Together, the dimers and trimers organize themselves in such a way as to create an active site cavity in the interior of the *PfM18AAP* assembly where the 12 monomer active sites are located in an equilateral triangle with distance  $\sim 33$  Å between them.

#### *Active site*

The *PfM18AAP* dodecamer contains four large pores, each  $\sim 23$  Å in diameter, which allow access to the active site cavity.<sup>120</sup> The disordered loop corresponding to residues 197-272 is thought to extend out over the entrance to the pores and so may serve to control substrate entry and enzyme function much akin to that seen in *PfA-M17*.<sup>105</sup> The individual  $S_1$  site of each monomer comprise an identical small cavity ( $\sim 23$  Å in diameter) lined by a host of polar residues (Glu380, Glu381, Gly509, Ser510, and His535) with Lys463 located at the bottom of the pocket. The positive charge of this Lys residue is ideally positioned to interact with the side chain of Asp and Glu of peptide substrates.<sup>121</sup> The two catalytic zinc ions are positioned immediately in front of the  $S_1$  cavity with one of the metal atoms coordinated by His87, Asp325 and Asp435, and the other coordinated by Asp325, Glu381 and His535.<sup>120</sup>

*PfM18AAP* is specific for the cleavage of acidic N-terminal residues

*PfM18AAP* exhibits a highly restricted substrate specificity as revealed when 60 natural and unnatural Xaa-ACC fluorogenic substrates were screened for enzymatic activity. Of these aminopeptidase substrates, only four (Glu-ACC, Asp-ACC, Asn-ACC, and the unnatural amino

acid DAP-ACC) were hydrolyzed.<sup>120,122</sup> *Pf*M18AAP displayed similar catalytic efficiency towards both Asp-ACC and Glu-ACC ( $k_{cat}/K_m$  values of  $360.1 \pm 28.5 \text{ M}^{-1} \text{ s}^{-1}$  and  $397.5 \pm 30.5 \text{ M}^{-1} \text{ s}^{-1}$  respectively), but was around 10-fold less efficient at cleaving Asn-ACC as a result of a much lower  $k_{cat}$ . DAP-ACC actually bound approximately seven times tighter to the enzyme than any of the three natural amino acids and showed the third best catalytic efficiency ( $k_{cat}/K_m = 96.6 \pm 8.5 \text{ M}^{-1} \text{ s}^{-1}$ ). It can be concluded that the role of *Pf*M18AAP is consistent with Hb degradation by facilitating the removal of acidic N-terminal amino acids which are unable to be cleaved by the other *Pf* aminopeptidases.

*Pf*M18AAP localizes to the parasite cytosol

*Pf*M18AAP is present in the cytosol of the parasite and is most highly expressed during the ring stage in the erythrocytic cycle.<sup>122</sup> A role of this cytosolic enzyme appears to be in the hydrolysis of Hb-derived short peptides generated in the PV and transported to the cytosolic space of the parasite. Since Hb contains around 8% Glu and Asp residues, *Pf*M18AAP is predicted make an important proteolytic contribution to the complete catabolism of Hb to free amino acids.

Development of inhibitors towards *Pf*M18AAP

The results of interfering with *Pf*M18AAP expression in blood stages of the parasite validate the aminopeptidase as a target for the development of antimalarial inhibitors. This enzyme does, however, present a challenge for the development of inhibitors in that the disordered loops extending out over the pores leading to the active site may block the access of inhibitor compounds. Nonetheless, a series of  $\alpha$ -phosphonic,  $\alpha$ -phosphinic, and phosphinate dipeptide derivatives of Asp and Glu have been designed and tested as inhibitors (Figure 20).<sup>122,123</sup> The derivatives of Glu were found to be the more potent inhibitors of the enzyme (e.g. **27**,  $K_i$ ,  $0.34 \mu\text{M}$ ), however none of the inhibitors were able to significantly inhibit the growth of the parasite in culture up to concentrations of  $100 \mu\text{M}$ .<sup>122</sup> Whilst these compounds may offer a potential starting point for

derivatization, extensive development would be required in order to produce an inhibitor capable of blocking parasite growth at a pharmacologically-relevant potency.

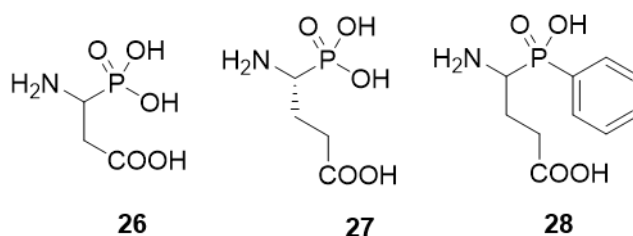


**Figure 20:**  $\alpha$ -Phosphonic derivatives of Asp (**26**) and Glu (**27**), and  $\alpha$ -phosphinic GluP-Ph (**28**). **27** was isolated as a single enantiomer, the other compounds were used as racemic mixtures.

More recently, a HTS of ~292,000 compounds from the Molecular Libraries Probe Production Centers Network (MLPCN) collection, the Molecular Libraries Small Molecule Repository (MLSMR), against *rPfM18AAP* was performed.<sup>124,125</sup> A cathepsin L1 (CTSL1) counter-screen was also implemented in order to remove non-specific inhibitors and fluorescence quenching molecules. Through several rounds of screening and counter-screening, the initial library of ~292,000 compounds yielded 125 hits that met the defined cut-off guidelines for selective inhibition of *rPfM18AAP*.<sup>124</sup> A subset of 76 of the 125 hits were resynthesized or purchased and subjected to a series of follow up assays to confirm inhibitory activity against: a) *rPfM18AAP*, b) malaria lysate aminopeptidase activity, and c) *Pf* parasite growth.<sup>124</sup> The outcome of these studies highlighted two potential lead compounds: CID6852389 (**29**), (*S*)-(+)-apomorphine hydrochloride hydrate; and CID23724194 (**30**), the hydrochloride salt of 4-[2-(acridin-9-ylamino)ethyl]benzene-1,2-diol (Figure 21).<sup>124</sup> Both of these compounds were found to be non-competitive inhibitors of *rPfM18AAP* with  $IC_{50}$  values of 4  $\mu$ M and 1.3  $\mu$ M, respectively, and showed inhibitory activity in an *in vitro* <sup>3</sup>H hypoxanthine incorporation growth assay with 87% and 96% growth inhibition at 10  $\mu$ M concentrations, respectively.<sup>124</sup>

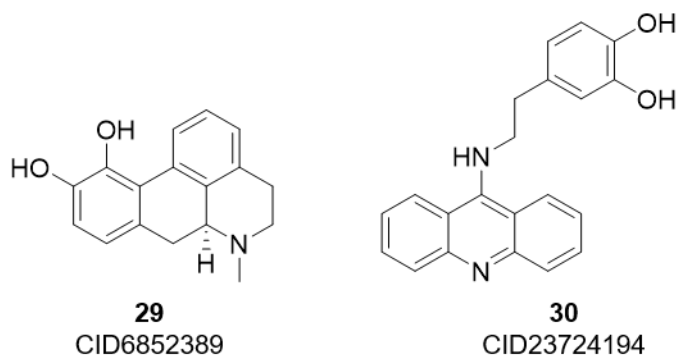


**Figure 21:** The catechol-containing inhibitors of *Pf*M18AAP identified *via* a HTS approach.<sup>124</sup>

Both **29** and **30** contain within their structure a reactive catechol moiety that has widely been described in pan-assay interference compounds (PAINS).<sup>126</sup> Nonetheless, the notion that these compounds were “false positives” has been rejected since the compounds were subjected to >100 different assays at various research facilities and neither compound was found to be active in any of the other assays. In conclusion, CID6852389 and CID23724194 have been proposed as potential new potent and selective inhibitors of *Pf*M18AAP and a starting point for the development of a novel antimalarial treatment.<sup>124</sup>

### Aminopeptidase P

Aminopeptidase P (APP), is a member of the M24 family of metalloproteases and has a specific role in the cleavage of N-terminal amino acids where the penultimate residue ( $P_1'$ ) is Pro.<sup>67,127</sup> These enzymes are typically cytoplasmic proteins and are found across a wide range of organisms. However, mammals also have an extracellular form of the enzyme (APP2) that is attached to the plasma membrane of cells by a glycosylphosphatidylinositol (GPI) anchor and has a role in the metabolism of peptides at the cell surface.<sup>128</sup> *Pf* possess a single 157 kDa cytosolic APP that has been studied in some detail and shown to be vital for parasite survival.<sup>36</sup>

The structure of *Pf*APP consists of three domains

#### *X-ray crystal structure*

Structure elucidation of *Pf*APP to 2.35 Å resolution revealed a homodimeric structure, with each monomer consisting of a three-domain arrangement (PDB ID: 5JQK).<sup>129</sup> Prior to the first domain, *Pf*APP contains a sequence of 120 residues which is not present in the mature form of the protein.<sup>37</sup> Domains I and II (residues 121-304 and 305-475 respectively) were found to be structurally similar, however, domain I exhibited a degree of flexibility and disorder within the crystal. Despite this, the crystal structure revealed secondary and quaternary structures of a seven-stranded  $\beta$ -sheet core surrounded by five helices.<sup>129</sup> *Pf*APP also has a 20-residue insertion from Tyr271-Val291 that is not included in the APP of other species.<sup>37</sup> This insertion forms one of the seven  $\beta$ -strands that make up the central core of this domain. Similar to domain I, domain II also has a central core structure comprising a six-stranded  $\beta$ -sheet core surrounded by five helices.

Domain III, the catalytic domain (residues 476-777), is comprised of two repeating  $\alpha\alpha\beta\beta\beta$  structures that are aligned in such a way as to create a 'pita-bread' fold.<sup>129</sup> This folded motif is common among the M24 family of aminopeptidase and prolidase enzymes across a range of species.<sup>130</sup> At the centre of this domain is a concave cavity in which lies the active site. Additionally, domain III contains the residues involved in forming the dimerization interface between the two monomers of *Pf*APP (Figure 22). The same residues from each monomer are involved in forming the critical contacts, meaning the dimerization is pseudo-symmetrical. Whilst hydrophobic interactions between the catalytic domains dominate the dimerization, salt bridges and hydrogen bonds also contribute. Two salt bridges are formed between residues Arg608 of one monomer and Glu629 on the opposite monomer. Two hydrogen bonds are also observed between Tyr617 and Asp637 of opposing monomers at the edge of the dimerization interface. Three identical Phe residues from each monomer (Phe625, Phe632 and Phe635) represent the driving

force of dimerization. Together, these six residues align themselves along the entire interface, and extend into cavities on the opposite monomer to form hydrophobic interactions. Phe625 interacts with Ile626, Ala622, Leu623, Thr618 and Val612; Phe632 with Ala615, Phe614 and Tyr706; Phe635 with the corresponding Ile613, the aliphatic chains of Lys398 and Glu699, and the ring of Tyr706.

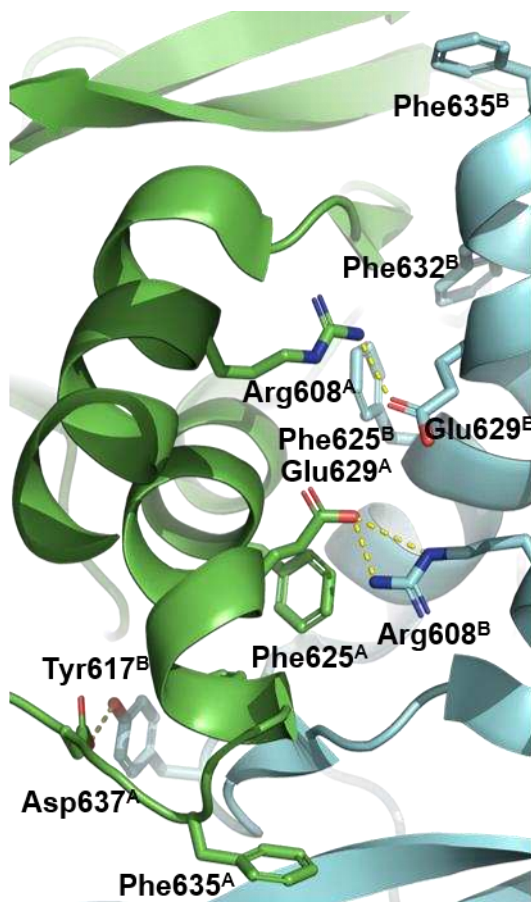


**Figure 22:** Dimerization interface between the two chains of *PfAPP* (PDB ID: 5JQK), colored according to chain (chain A colored green, chain B colored blue).<sup>129</sup> The key residues involved in forming the dimerization contacts are shown as sticks and labeled accordingly. Electrostatic interactions between the dimerization residues are displayed as yellow dashed lines. Image generated using PyMOL.<sup>102</sup>

### *Active site*

The *PfAPP* active site is located in domain III and is linked to two openings: one extends into the interior of the dimer structure, whereas the second extends out to the exterior of the enzyme.<sup>129</sup> The second opening (~10 Å wide) is narrower than the first and is formed *via* the interface between the three domains. Two active site manganese (II) ions (Mn1 and Mn2) are known to be involved in catalysis.<sup>37,131,132</sup> Mn1 is coordinated by Asp570, Asp581, Glu690, whereas Mn2 is coordinated by Glu676, His644, Asp581, Glu690.<sup>129</sup>

The *PfAPP* active site is highly specific for the cleavage of Xaa-Pro bonds

APP specifically cleaves the N-terminal amino acid from peptides with Pro in the P<sub>1</sub>' position. The Xaa-Pro peptide bond is resistant to hydrolysis by peptidases with broad substrate specificity as a consequence of the conformational rigidity conferred by the Pro side chain that is part of a five-membered ring that includes both the C $\alpha$  and the amino nitrogen atom.<sup>127</sup> *PfAPP* is the only malaria parasite peptidase known to cleave Xaa-Pro substrates, thus supporting the hypotheses that the enzyme plays a critical role in Hb catabolism and parasite survival.<sup>36,129</sup>

*PfAPP* localizes to both the parasite cytosol and the food vacuole

*PfAPP* is unique in respect to most other *PfMAPs* in that it is localized to both the FV and the cytosol of the parasite, suggesting catabolic roles in these locations, a view supported by the demonstration of strong catalytic activity at both the acidic (pH 5.5) and neutral (pH 7.5) pH of the respective compartment environments.<sup>36,37</sup> In contrast, human cytosolic APP1 is rather unstable at pH 5.5.<sup>85</sup>

Development of inhibitors towards *PfAPP*

Apstatin (**31**, Figure 23), a short peptide inhibitor of both human APP and *PfAPP* comprises a tripeptide and the N-terminal (2*S*,3*R*)-3-amino-2-hydroxy-4-phenyl-butanoic acid (AHPB) group of bestatin.<sup>129,133–136</sup> The tripeptide sequence is based on the specificity of APP for Pro in the P<sub>1</sub>'

position, and the increased inhibition observed from a tetrapeptide sequence. Apstatin was determined to be a weak inhibitor of *Pf*APP, with  $IC_{50}$  value of  $20.2 \pm 1.2 \mu\text{M}$  that is similar to that reported for human APP1 and APP2.<sup>129</sup>

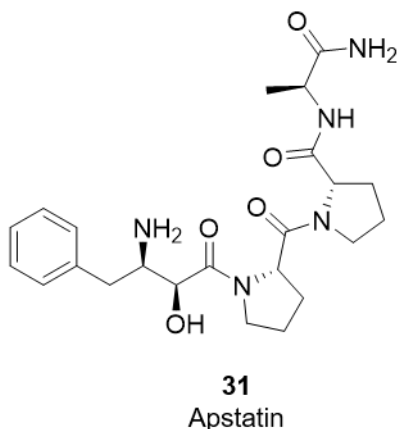


**Figure 23:** Apstatin.<sup>129</sup>

The crystal structure of apstatin bound to *Pf*APP (Figure 24, PDB ID: 5JR6) has also been solved.<sup>129</sup> The hydroxyl group of the AHPB binds to both catalytic Mn(II) ions at the active site and the carbonyl group between the  $P_1$  and  $P_1'$  residues interacts with His653. It was found that the  $S_1'$  subsite of *Pf*APP is highly optimized for the binding of Pro: three His residues (His640, His653 and His551) shape this site, introducing a slight bend in the binding site between the  $S_1$  and  $S_1'$  pockets, making it specific for Pro.<sup>129</sup> There are no discernible interactions between the enzyme and apstatin at, and beyond, the  $S_2'$  subsite indicating a less defined and more open substrate binding site at this point. Improving the interactions made between the inhibitor and *Pf*APP in the  $S_2'$  and  $S_3'$  subsites may offer opportunities to improve inhibitor potency.

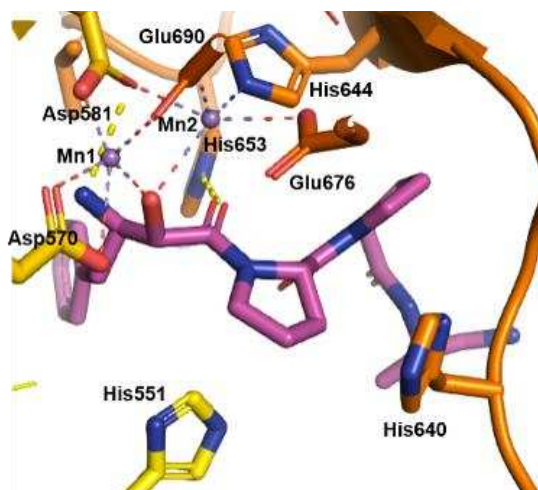


**Figure 24:** Binding pose of apstatin (**31**, purple) in the active site of *PfAPP* (PDB ID: 5JR6). The molecules are colored according to atom. The catalytic Mn(II) ions are shown as blue spheres. Polar interactions are indicated by yellow dashed lines. Interactions between the Mn(II) ions and the inhibitor or the enzyme are shown as multi-colored dashed lines. Image generated using PyMOL.<sup>102</sup>

*PfAPP* is clearly an attractive target for inhibitor development because it is essential for parasite survival, however apstatin is a relatively weak inhibitor and, as yet, a more potent analogue of **31** has not been developed.

#### *Selectivity*

Achieving inhibitor selectivity between *PfAPP* and the human APP orthologs (cytosolic hAPP1 and the ectopeptidase hAPP2) is an important objective, but may present a significant challenge since the catalytic domains of *PfAPP* and hAPP1 are well conserved.<sup>129</sup> This includes conserved S<sub>1</sub> and S<sub>1</sub>' subsites, as well as an identical di-metal ion arrangement. The X-ray crystal structure of *PfAPP* in complex with apstatin identifies the binding mode of the inhibitor, but the crystal structure of hAPP1 in complex with apstatin has not yet been solved. Despite this, differences in the properties of the S<sub>2</sub>' subsites have been identified which may offer the potential for realizing

selective inhibitor design.<sup>129</sup> In hAPP1, a ten-residue loop on the periphery of the dimerization interface directs Lys507 into the S<sub>2</sub>' binding subsite. In contrast, the equivalent loop in *Pf*APP is only eight residues in length and is positioned further from the binding site. As a result of this, the P<sub>2</sub>' Pro of apstatin and Lys507 present a clash when the binding pose generated from the apstatin:*Pf*APP crystal structure was placed into the hAPP1 binding site.<sup>129</sup> In addition, hAPP2 is unable to cleave substrates with bulky P<sub>2</sub>' residues. This observation suggests that inhibitor selectivity could be introduced through tuning of the P<sub>2</sub>' residue.<sup>129</sup>

### Directions for future progress

The need for new antimalarial drugs is urgent to combat the appearance of drug-resistant strains of *Pf* parasites that threaten the effectiveness of current therapeutic approaches. The gold-standard for treatment of *Pf* malaria involves the use of ACTs and has been successfully implemented for many years. The emergence of resistance to ACTs in South-East Asia, and, more recently Africa, presents a significant challenge for controlling the burden of malaria.<sup>13,137</sup> Should the efficacy of ACTs become significantly reduced, there are currently no replacement therapies against *Pf* malaria.

To address the increasing concerns about drug resistance, new antimalarials are required with novel modes of action to minimise the risk of cross-resistance. Release of the *Pf* malaria genome sequence in 2002 has provided a wealth of genomic information of value in selecting potential new target proteins, primarily enzymes and membrane transporter proteins, for molecular characterization and validation.<sup>46</sup> The vital role of proteases in providing Hb-derived amino acids for parasite protein synthesis during the erythrocytic stages of the malaria life-cycle has attracted much attention to these enzymes as druggable targets. Importantly, protease catalytic mechanisms

are well understood and can be readily exploited in the design of selective inhibitors. *Pf* aminopeptidases play critical roles in the final stages of converting Hb-derived peptides to free amino acids for parasite protein synthesis, and several have been validated as promising targets.<sup>46</sup> Work in recent years producing active recombinant forms of the aminopeptidases and solving the X-ray crystal structures has also enabled a more guided and focused approach to drug development. In addition, the development of robust *in vitro* assay procedures and small animal models in order to study the effectiveness of new antimalarial agents has been a major step forward in the drug development process.<sup>138</sup>

Previously, antimalarial drugs have been identified through the use of *in vitro* or animal models and so the exact target of the drug is unknown.<sup>4</sup> As such, the mechanisms for development of resistance are also not fully understood. In order to prevent this in the future, a more rational approach to development of inhibitors against a known target is the preferred strategy. While a number of inhibitors against the various aminopeptidases have been identified to date, many display limitations in areas such as *in vitro* potency, PK parameters and host toxicity. Nonetheless, the recent progress made in the characterization of critical *Pf* proteases, especially the metalloaminopeptidases, and the identification of potent inhibitors bodes well for the development of small molecule inhibitors as the basis for novel antimalarial therapies against drug-resistant strains. Recent advances in artificial intelligence (AI) and machine learning (ML) techniques may prove important computational tools for the future development of antimalarials.<sup>139</sup> AI has already found success in identifying promising drug compounds to treat diseases such as cancer and motor neurone disease.<sup>140</sup> Use of these techniques could reduce the time and costs of the drug discovery process, along with reducing the rate of drug attrition and improving overall efficiency by enabling more accurate predictions of PK parameters and toxicity.<sup>139,141</sup>

Due to the ability of *Pf* parasites to rapidly develop resistance against antimalarial drugs there has been increased interest in developing drugs with novel mechanisms of action, which can be used in combination therapy to reduce the risk for the development of resistance towards them. The development of hybrid inhibitors of the *PfA-M1* and *PfA-M17* aminopeptidases, such as those described in figures 18 and 19, illustrates the potential for this strategy. Here, the similarity between the enzyme substrate specificities has been exploited for the development of hybrid inhibitors and since both enzymes have been proven vital for parasite survival, inhibition of both enzymes with a single drug compound represents a highly desirable strategy for antimalarial drug development.

A major factor which has slowed the development of novel antimalarial drugs is the large discrepancy often seen between the potency of the inhibitor against the free enzyme and the potency against parasite growth. This issue has been noted in several studies highlighted within this review and is a trend which is not fully understood. There have been suggestions as to why this occurs, including poor permeability of the inhibitor limiting the uptake of the drug and thus preventing it from reaching the site of action, however this has been found to not always be the case and requires further investigations to aid the development of new antimalarials.

In April of this year, the World Health Organization (WHO) Strategic Advisory Group on Malaria Eradication (SAGme) published a report highlighting six key areas which are fundamental for the eradication of malaria.<sup>142</sup> These areas included: reinforcing the *Global technical strategy for malaria 2016-2030*; research and development for new tools; access to affordable, high quality, people-centered health care and services; adequate and sustained financing; strengthened surveillance and response; and engaging communities. Whilst these strategies alone will not

eradicate malaria, the implementation of strategies to aid in the fight against malaria in conjunction with new antimalarial drugs and vaccines is key to achieve the goal of malaria eradication.

## Conclusion

The emergence of resistance to current treatments has led to significant interest in the development of novel antimalarial drugs. One area which has been highlighted as providing promising targets for novel therapies is the inhibition of the malaria parasite MAPs. Within *Pf*, the MAPs are believed to have an essential biological role and so inhibition of these enzymes presents an attractive strategy for combatting drug-resistant malarial species. Production of functionally active recombinant constructs of these aminopeptidases, along with their corresponding X-ray crystal structures have enabled for detailed structural analysis to be carried out. In addition to this, analysis of the active site architecture has enabled for a more rational approach to drug design and optimisation of inhibitors. In some cases, knowledge of the active site structure of the malarial enzyme and the corresponding human ortholog has allowed for investigations into designing selective inhibitors towards the parasite. In the case of *PfA-M1* and *PfA-M17* in particular, the identification of a basic core, around which a series of optimizations have been undertaken, has allowed for the identification of potent and selective lead compounds. The possibility of developing a potent, selective inhibitor towards one (or more) of the malarial MAPs remains an attractive approach to developing novel antimalarial drugs.

Author information

### Corresponding author

\*E-mail: r.foster@leeds.ac.uk

## Biographies

**Richard Foster** received a B.Sc. in Chemistry and a Ph.D. in Organic Chemistry from the University of Leeds, UK. He joined Tripos Discovery Research in 1998, and in 2008, he moved to the University of Leeds where he is currently Associate Professor of Medicinal Chemistry. Richard has led medicinal chemistry efforts directed at various anti-malarial, cardiovascular, metabolic, and inflammatory targets. He is the scientific founder of LUNAC Therapeutics, a cardiovascular drug development company, focused on the discovery of novel antithrombotic therapies. He has co-authored over 60 peer-reviewed publications and patents.

**Belinda Mills** received her MChem in Medicinal Chemistry from the University of Leeds in 2018 where she was awarded the Craig Jordan Medicinal Chemistry prize. She is currently in the second year of her Medical Research Council funded PhD in the group of Dr Richard Foster and co-supervised by Professor Elwyn Isaac at the University of Leeds. Her research interests lie in the field of medicinal chemistry, with particular interest in the development of small molecule aminopeptidase inhibitors.

**Elwyn Isaac** graduated with a B. Sc. and Ph. D. in Biochemistry from Cardiff University, Wales, U.K. He joined the group of H.H. Rees and T.W Goodwin at Liverpool University working on the biosynthesis and structure of insect steroids before joining the University of Leeds as a lecturer in 1984. He has held the position of Professor of Comparative Biochemistry at the Faculty of Biological Sciences, University of Leeds, since 2002 and has published extensively on the biochemistry of metallopeptidases belonging to the neprilysin, angiotensin converting enzyme (ACE) and aminopeptidase families.

## Acknowledgments

The authors would like to thank the Medical Research Council (MRC) for providing the financial support.

#### Abbreviations

ACC, 7-amino-4-carbamoylmethylcoumarin; ACTs, Artemisinin-based combination therapies; AHPB, (2*S*,3*R*)-3-Amino-2-hydroxy-4-phenyl-butanoic acid; AI, Artificial Intelligence; APP, Aminopeptidase P; BES, Bestatin; CQ, Chloroquine; CTSL1, Cathepsin L1; DAP, 2,3-Diaminopropionic acid; *EcPepN*, *E. coli* Aminopeptidase N; EDTA, Ethylenediaminetetraacetic acid; FV, Food Vacuole; GPI, Glycosylphosphatidylinositol; GSK, GlaxoSmithKline; hAPN, Human Aminopeptidase N; hAPP1, Human Aminopeptidase P 1; hAPP2, Human Aminopeptidase P 2; Hb, Hemoglobin; HEK293, Human Embryonic Kidney Cells; HuMetAP2, Human Methionine Aminopeptidase 2; HTS, High-Throughput Screen; IRAP, Insulin-Regulated Aminopeptidase; LAPs, Leucyl Aminopeptidases; MAP, Metalloaminopeptidase; MetAP, Methionine Aminopeptidase; ML, Machine Learning; MLPCN, Molecular Libraries Probe Production Centers Network; MLSMR, Molecular Libraries Small Molecule Repository; MMP, Matrix Metalloproteinase; NTE, N-Terminal Extension; PAINS, Pan Assay Interference Compounds; PDB, Protein Data Bank; *Pf*, *Plasmodium falciparum*; *PfA-M1*, *Plasmodium falciparum* Alanine Aminopeptidase; *PfA-M17*, *Plasmodium falciparum* Leucyl Aminopeptidase; *PfAPP*, *Plasmodium falciparum* Aminopeptidase P; *PfCRT*, *Plasmodium falciparum* Chloroquine Resistance Transporter; *PfDPAP1*, *Plasmodium falciparum* Dipeptidyl Aminopeptidase 1; *PfFP-2*, *Plasmodium falciparum* Falcipain 2; *PfFP-2'*, *Plasmodium falciparum* Falcipain 2'; *PfFP-3*, *Plasmodium falciparum* Falcipain 3; *PfHAP*, *Plasmodium falciparum* Histoaspartic Proteinase; *PfM18AAP*, *Plasmodium falciparum* Aspartyl Aminopeptidase; *Pfmdr1*, *Plasmodium falciparum* Multidrug Resistance 1; *PfMetAP1a*, *Plasmodium falciparum* Methionine Aminopeptidase 1a;

*PfMetAP1b*, *Plasmodium falciparum* Methionine Aminopeptidase 1b; *PfMetAP1c*, *Plasmodium falciparum* Methionine Aminopeptidase 1c; *PfMetAP2*, *Plasmodium falciparum* Methionine Aminopeptidase 2; *PfPM1*, *Plasmodium falciparum* Plasmepsin 1; *PfPM2*, *Plasmodium falciparum* Plasmepsin 2; *PfPM4*, *Plasmodium falciparum* Plasmepsin 4; PK, Pharmacokinetic; *Pv*, *Plasmodium vivax*; PV, Parasitophorous Vacuole; RBC, Red Blood Cell; SAGme, Strategic Advisory Group on Malaria Eradication; SAR, Structure Activity Relationship; WHO, World Health Organization; WRAIR, Walter Reed Army Institute of Research; YFP, Yellow Fluorescent Protein.

## References

- (1) World Health Organization. *World Malaria Report 2020*; Geneva, 2020.
- (2) Centers for Disease Control and Prevention <https://www.cdc.gov/> (accessed Jun 3, 2020).
- (3) Hemingway, J.; Ranson, H.; Magill, A.; Kolaczinski, J.; Fornadel, C.; Gimnig, J.; Coetzee, M.; Simard, F.; Roch, D. K.; Hinzoumbe, C. K.; Pickett, J.; Schellenberg, D.; Gething, P.; Hoppé, M.; Hamon, N. Averting a Malaria Disaster: Will Insecticide Resistance Derail Malaria Control? *Lancet* **2016**, *387*, 1785–1788.
- (4) Kumar, S.; Bhardwaj, T. R.; Prasad, D. N.; Singh, R. K. Drug Targets for Resistant Malaria: Historic to Future Perspectives. *Biomed. Pharmacother.* **2018**, *104*, 8–27.
- (5) Price, R. N.; Cassar, C.; Brockman, A.; Duraisingh, M.; Van Vugt, M.; White, N. J.; Nosten, F.; Krishna, S. The *Pfmdr1* Gene Is Associated with a Multidrug-Resistant Phenotype in *Plasmodium Falciparum* from the Western Border of Thailand. *Antimicrob. Agents Chemother.* **1999**, *43*, 2943–2949.

- (6) Sidhu, A. B. S.; Uhlemann, A.; Valderramos, S. G.; Valderramos, J.; Krishna, S.; Fidock, D. A. Decreasing Pfmdr1 Copy Number in Plasmodium Falciparum Malaria Heightens Susceptibility to Mefloquine, Lumefantrine, Halofantrine, Quinine, and Artemisinin. *J. Infect. Dis.* **2006**, *194*, 528–535.
- (7) Syafruddin, D.; Siregar, J. E.; Marzuki, S. Mutations in the Cytochrome b Gene of Plasmodium Berghei Conferring Resistance to Atovaquone. *Mol. Biochem. Parasitol.* **1999**, *104*, 185–194.
- (8) Plowe, C. V.; Kublin, J. G.; Doumbo, O. K. P. Falciparum Dihydrofolate Reductase and Dihydropteroate Synthase Mutations: Epidemiology and Role in Clinical Resistance to Antifolates. *Drug Resist. Updat.* **1998**, *1*, 389–396.
- (9) Fidock, D. A.; Nomura, T.; Talley, A. K.; Cooper, R. A.; Dzekunov, S. M.; Ferdig, M. T.; Ursos, L. M. B.; Bir Singh Sidhu, A.; Naudé, B.; Deitsch, K. W.; Su, X. Z.; Wootton, J. C.; Roepe, P. D.; Wellems, T. E. Mutations in the P. Falciparum Digestive Vacuole Transmembrane Protein PfCRT and Evidence for Their Role in Chloroquine Resistance. *Mol. Cell* **2000**, *6*, 861–871.
- (10) Slater, A. F. G. Chloroquine: Mechanism of Drug Action and Resistance in Plasmodium Falciparum. *Pharmacol. Ther.* **1993**, *57*, 203–235.
- (11) Wellems, T. E.; Plowe, C. V. Chloroquine-Resistant Malaria. *J. Infect. Dis.* **2001**, *184*, 770–776.
- (12) Rieckmann, K. H.; Davis, D. R.; Hutton, D. C. Plasmodium Vivax Resistance to Chloroquine? *Lancet* **1989**, *334*, 1183–1184.

- (13) Eastman, R. T.; Fidock, D. A. Artemisinin-Based Combination Therapies: A Vital Tool in Efforts to Eliminate Malaria. *Nat. Rev. Microbiol.* **2009**, *7*, 864–874.
- (14) Cui, L.; Mharakurwa, S.; Ndiaye, D.; Rathod, P. K.; Rosenthal, P. J. Antimalarial Drug Resistance: Literature Review and Activities and Findings of the ICEMR Network. *Am. J. Trop. Med. Hyg* **2015**, *93*, 57–68.
- (15) Ferreira, M. U.; Nobrega de Sousa, T.; Rangel, G. W.; Johansen, I. C.; Corder, R. M.; Ladeia-Andrade, S.; Gil, J. P. Monitoring Plasmodium Vivax Resistance to Antimalarials: Persisting Challenges and Future Directions. *Int. J. Parasitol. Drugs Drug Resist.* **2021**, *15*, 9-24.
- (16) Price, R. N.; von Seidlein, L.; Valecha, N.; Nosten, F.; Baird, J. K.; White, N. J. Global Extent of Chloroquine-Resistant Plasmodium Vivax: A Systematic Review and Meta-Analysis. *Lancet Infect. Dis.* **2014**, *14*, 982–991.
- (17) Ashley, E. A.; Dhorda, M.; Fairhurst, R. M.; Amaratunga, C.; Lim, P.; Suon, S.; Sreng, S.; Anderson, J. M.; Mao, S.; Sam, B.; Sopha, C.; Chuor, C. M.; Nguon, C.; Sovannaroeth, S.; Pukrittayakamee, S.; Jittamala, P.; Chotivanich, K.; Chutasmit, K.; Suchatsoonthorn, C.; Runcharoen, R.; Hien, T. T.; Thuy-Nhien, N. T.; Thanh, N. V.; Phu, N. H.; Htut, Y.; Han, K.-T.; Aye, K. H.; Mokuolu, O. A.; Olaosebikan, R. R.; Folaranmi, O. O.; Mayxay, M.; Khanthavong, M.; Hongvanthong, B.; Newton, P. N.; Onyamboko, M. A.; Fanello, C. I.; Tshefu, A. K.; Mishra, N.; Valecha, N.; Phyto, A. P.; Nosten, F.; Yi, P.; Tripura, R.; Borrmann, S.; Bashraheil, M.; Peshu, J.; Faiz, M. A.; Ghose, A.; Hossain, M. A.; Samad, R.; Rahman, M. R.; Hasan, M. M.; Islam, A.; Miotto, O.; Amato, R.; MacInnis, B.; Stalker, J.; Kwiatkowski, D. P.; Bozdech, Z.; Jeeyapant, A.; Cheah, P. Y.; Sakulthaew, T.; Chalk,

- J.; Intharabut, B.; Silamut, K.; Lee, S. J.; Vihokhern, B.; Kunasol, C.; Imwong, M.; Tarning, J.; Taylor, W. J.; Yeung, S.; Woodrow, C. J.; Flegg, J. A.; Das, D.; Smith, J.; Venkatesan, M.; Plowe, C. V.; Stepniewska, K.; Guerin, P. J.; Dondorp, A. M.; Day, N. P.; White, N. J. Spread of Artemisinin Resistance in *Plasmodium Falciparum* Malaria. *N. Engl. J. Med.* **2014**, *371*, 411–423.
- (18) Laurens, M. B. RTS,S/AS01 Vaccine (Mosquirix™): An Overview. *Hum. Vaccines Immunother.* **2020**, *16*, 480–489.
- (19) Alonso, P. L.; Sacarlal, J.; Aponte, J. J.; Leach, A.; Macete, E.; Milman, J.; Mandomando, I.; Spiessens, B.; Guinovart, C.; Espasa, M.; Bassat, Q.; Aide, P.; Ofori-Anyinam, O.; Navia, M. M.; Corachan, S.; Ceuppens, M.; Dubois, M. C.; Demoitié, M. A.; Dubovsky, F.; Menéndez, C.; Tornieporth, N.; Ballou, W. R.; Thompson, R.; Cohen, J. Efficacy of the RTS,S/AS02A Vaccine against Plasmodium Falciparum Infection and Disease in Young African Children: Randomised Controlled Trial. *Lancet* **2004**, *364*, 1411–1420.
- (20) Bejon, P.; White, M. T.; Olotu, A.; Bojang, K.; Lusingu, J. P. A.; Salim, N.; Otsyula, N. N.; Agnandji, S. T.; Asante, K. P.; Owusu-Agyei, S.; Abdulla, S.; Ghani, A. C. Efficacy of RTS,S Malaria Vaccines: Individual-Participant Pooled Analysis of Phase 2 Data. *Lancet Infect. Dis.* **2013**, *13*, 319–327.
- (21) Aponte, J. J.; Aide, P.; Renom, M.; Mandomando, I.; Bassat, Q.; Sacarlal, J.; Manaca, M. N.; Lafuente, S.; Barbosa, A.; Leach, A.; Lievens, M.; Vekemans, J.; Sigauque, B.; Dubois, M. C.; Demoitié, M. A.; Sillman, M.; Savarese, B.; McNeil, J. G.; Macete, E.; Ballou, W. R.; Cohen, J.; Alonso, P. L. Safety of the RTS,S/AS02D Candidate Malaria Vaccine in Infants Living in a Highly Endemic Area of Mozambique: A Double Blind Randomised

- Controlled Phase I/IIb Trial. *Lancet* **2007**, *370*, 1543–1551.
- (22) RTS, S. C. T. P. Efficacy and Safety of RTS,S/AS01 Malaria Vaccine with or without a Booster Dose in Infants and Children in Africa: Final Results of a Phase 3, Individually Randomised, Controlled Trial. *Lancet* **2015**, *386*, 31–45.
- (23) Trenholme, K. R.; Brown, C. L.; Skinner-Adams, T. S.; Stack, C.; Lowther, J.; To, J.; Robinson, M. W.; Donnelly, S. M.; Dalton, J. P.; Gardiner, D. L. Aminopeptidases of Malaria Parasites: New Targets for Chemotherapy. *Infect. Disord. - Drug Targets* **2010**, *10*, 217–225.
- (24) Bozdech, Z.; Llinás, M.; Pulliam, B. L.; Wong, E. D.; Zhu, J.; DeRisi, J. L. The Transcriptome of the Intraerythrocytic Developmental Cycle of *Plasmodium Falciparum*. *PLoS Biol.* **2003**, *1*, e5.
- (25) Goldberg, D. E.; Slater, A. F. G.; Cerami, A.; Henderson, G. B. Hemoglobin Degradation in the Malaria Parasite *Plasmodium Falciparum*: An Ordered Process in a Unique Organelle. *Proc. Natl. Acad. Sci. U. S. A.* **1990**, *87*, 2931–2935.
- (26) Coombs, G. H.; Goldberg, D. E.; Klemba, M.; Berry, C.; Kay, J.; Mottram, J. C. Aspartic Proteases of *Plasmodium Falciparum* and Other Parasitic Protozoa as Drug Targets. *Trends Parasitol.* **2001**, *17*, 532–537.
- (27) Banerjee, R.; Liu, J.; Beatty, W.; Pelosof, L.; Klemba, M.; Goldberg, D. E. Four Plasmepsins Are Active in the *Plasmodium Falciparum* Food Vacuole, Including a Protease with an Active-Site Histidine. *Proc. Natl. Acad. Sci. U. S. A.* **2002**, *99*, 990–995.
- (28) Klemba, M.; Goldberg, D. E. Characterization of Plasmepsin V, a Membrane-Bound

- Aspartic Protease Homolog in the Endoplasmic Reticulum of Plasmodium Falciparum. *Mol. Biochem. Parasitol.* **2005**, *143*, 183–191.
- (29) Goldberg, D. E.; Slater, A. F. G.; Beavis, R.; Chait, B.; Cerami, A.; Henderson, G. B. Hemoglobin Degradation in the Human Malaria Pathogen Plasmodium Falciparum: A Catabolic Pathway Initiated by a Specific Aspartic Protease. *J. Exp. Med.* **1991**, *173*, 961–969.
- (30) Gluzman, I. Y.; Francis, S. E.; Oksman, A.; Smith, C. E.; Duffin, K. L.; Goldberg, D. E. Order and Specificity of the Plasmodium Falciparum Hemoglobin Degradation Pathway. *J. Clin. Invest.* **1994**, *93*, 1602–1608.
- (31) Drew, M. E.; Banerjee, R.; Uffman, E. W.; Gilbertson, S.; Rosenthal, P. J.; Goldberg, D. E. Plasmodium Food Vacuole Plasmepsins Are Activated by Falcipains. *J. Biol. Chem.* **2008**, *283*, 12870–12876.
- (32) Eggleston, K. K.; Duffin, K. L.; Goldberg, D. E. Identification and Characterization of Falcilysin, a Metallopeptidase Involved in Hemoglobin Catabolism within the Malaria Parasite Plasmodium Falciparum. *J. Biol. Chem.* **1999**, *274*, 32411–32417.
- (33) Klemba, M.; Gluzman, I.; Goldberg, D. E. A Plasmodium Falciparum Dipeptidyl Aminopeptidase I Participates in Vacuolar Hemoglobin Degradation. *J. Biol. Chem.* **2004**, *279*, 43000–43007.
- (34) Tanaka, T. Q.; Deu, E.; Molina-Cruz, A.; Ashburne, M. J.; Ali, O.; Suri, A.; Kortagere, S.; Bogyo, M.; Williamson, K. C. Plasmodium Dipeptidyl Aminopeptidases as Malaria Transmission-Blocking Drug Targets. *Antimicrob. Agents Chemother.* **2013**, *57*, 4645–

4652.

- (35) Gavigan, C. S.; Dalton, J. P.; Bell, A. The Role of Aminopeptidases in Haemoglobin Degradation in Plasmodium Falciparum-Infected Erythrocytes. *Mol. Biochem. Parasitol.* **2001**, *117*, 37–48.
- (36) Dalal, S.; Klemba, M. Roles for Two Aminopeptidases in Vacuolar Hemoglobin Catabolism in Plasmodium Falciparum. *J. Biol. Chem.* **2007**, *282*, 35978–35987.
- (37) Ragheb, D.; Bompiani, K.; Dalal, S.; Klemba, M. Evidence for Catalytic Roles for Plasmodium Falciparum Aminopeptidase P in the Food Vacuole and Cytosol. *J. Biol. Chem.* **2009**, *284*, 24806–24815.
- (38) Harbut, M. B.; Velmourougane, G.; Dalal, S.; Reiss, G.; Whisstock, J. C.; Onder, O.; Brisson, D.; McGowan, S.; Klemba, M.; Greenbaum, D. C. Bestatin-Based Chemical Biology Strategy Reveals Distinct Roles for Malaria M1- and M17-Family Aminopeptidases. *Proc. Natl. Acad. Sci. U. S. A.* **2011**, *108*, E526–E534.
- (39) Azimzadeh, O.; Sow, C.; Gèze, M.; Nyalwidhe, J.; Florent, I. Plasmodium Falciparum PfA-M1 Aminopeptidase Is Trafficked via the Parasitophorous Vacuole and Marginally Delivered to the Food Vacuole. *Malar. J.* **2010**, *9*. DOI: [10.1186/1475-2875-9-189](https://doi.org/10.1186/1475-2875-9-189).
- (40) Pagola, S.; Stephens, P. W.; Bohle, D. S.; Kosar, A. D.; Madsen, S. K. The Structure of Malaria Pigment  $\beta$ -Haematin. *Nature* **2000**, *404*, 307–310.
- (41) Egan, T. J.; Combrinck, J. M.; Egan, J.; Hearne, G. R.; Marques, H. M.; Ntenti, S.; Sewell, B. T.; Smith, P. J.; Taylor, D.; Van Schalkwyk, D. A.; Walden, J. C. Fate of Haem Iron in the Malaria Parasite Plasmodium Falciparum. *Biochem. J.* **2002**, *365*, 343–347.

- (42) Omara-Opyene, A. L.; Moura, P. A.; Sulsona, C. R.; Bonilla, J. A.; Yowell, C. A.; Fujioka, H.; Fidock, D. A.; Dame, J. B. Genetic Disruption of the Plasmodium Falciparum Digestive Vacuole Plasmepsins Demonstrates Their Functional Redundancy. *J. Biol. Chem.* **2004**, *279*, 54088–54096.
- (43) Liu, J.; Istvan, E. S.; Gluzman, I. Y.; Gross, J.; Goldberg, D. E. Plasmodium Falciparum Ensures Its Amino Acid Supply with Multiple Acquisition Pathways and Redundant Proteolytic Enzyme Systems. *Proc. Natl. Acad. Sci. U. S. A.* **2006**, *103*, 8840–8845.
- (44) Lin, J. wen; Spaccapelo, R.; Schwarzer, E.; Sajid, M.; Annoura, T.; Deroost, K.; Ravelli, R. B. G.; Aime, E.; Capuccini, B.; Mommaas-Kienhuis, A. M.; O’Toole, T.; Prins, F.; Franke-Fayard, B. M. D.; Ramesar, J.; Chevalley-Maurel, S.; Kroeze, H.; Koster, A. J.; Tanke, H. J.; Crisanti, A.; Langhorne, J.; Arese, P.; Van den Steen, P. E.; Janse, C. J.; Khan, S. M. Replication of Plasmodium in Reticulocytes Can Occur without Hemozoin Formation, Resulting in Chloroquine Resistance. *J. Exp. Med.* **2015**, *212*, 893–903.
- (45) Schechter, I.; Berger, A. On the Size of the Active Site in Proteases. I. Papain. *Biochem. Biophys. Res. Commun.* **1967**, *27*, 157–162.
- (46) Gardner, M. J.; Hall, N.; Fung, E.; White, O.; Berriman, M.; Hyman, R. W.; Carlton, J. M.; Pain, A.; Nelson, K. E.; Bowman, S.; Paulsen, I. T.; James, K.; Eisen, J. A.; Rutherford, K.; Salzberg, S. L.; Craig, A.; Kyes, S.; Chan, M.-S.; Nene, V.; Shallom, S. J.; Suh, B.; Peterson, J.; Angiuoli, S.; Pertea, M.; Allen, J.; Selengut, J.; Haft, D.; Mather, M. W.; Vaidya, A. B.; Martin, D. M. A.; Fairlamb, A. H.; Fraunholz, M. J.; Roos, D. S.; Ralph, S. A.; Mcfadden, G. I.; Cummings, L. M.; Subramanian, G. M.; Mungall, C.; Venter, J. C.; Carucci, D. J.; Hoffman, S. L.; Newbold, C.; Davis, R. W.; Fraser, C. M.; Barrell, B. Genome Sequence

- of the Human Malaria Parasite *Plasmodium Falciparum* Europe PMC Funders Group.  
*Nature* **2002**, *419*, 498-511.
- (47) PlasmoDB [www.plasmodb.org](http://www.plasmodb.org) (accessed Dec 10, 2020).
- (48) da Silva, F. L.; Dixon, M. W. A.; Stack, C. M.; Teuscher, F.; Taran, E.; Jones, M. K.; Lovas, E.; Tilley, L.; Brown, C. L.; Trenholme, K. R.; Dalton, J. P.; Gardiner, D. L.; Skinner-Adams, T. S. A *Plasmodium Falciparum* S33 Proline Aminopeptidase Is Associated with Changes in Erythrocyte Deformability. *Exp. Parasitol.* **2016**, *169*, 13–21.
- (49) Yoshimoto, T.; Kabashima, T.; Uchikawa, K.; Inoue, T.; Tanaka, N.; Nakamura, K. T.; Tsuru, M.; Ito, K. Crystal Structure of Prolyl Aminopeptidase from *Serratia Marcescens*. *J. Biochem.* **1999**, *126*, 559–565.
- (50) Bolumar, T.; Sanz, Y.; Aristoy, M.-C.; Toldrá, F. Purification and Characterization of a Prolyl Aminopeptidase from *Debaryomyces Hansenii*. *Appl. Environ. Microbiol.* **2003**, *69*, 227–232.
- (51) Battle, K. E.; Gething, P. W.; Elyazar, I. R. F.; Moyes, C. L.; Sinka, M. E.; Howes, R. E.; Guerra, C. A.; Price, R. N.; Baird, K. J.; Hay, S. I. The Global Public Health Significance of *Plasmodium Vivax*. In *Advances in Parasitology*; Academic Press, 2012; Vol. 80, pp 1–111.
- (52) Rout, S.; Mahapatra, R. K. In Silico Study of M18 Aspartyl Amino Peptidase (M18AAP) of *Plasmodium Vivax* as an Antimalarial Drug Target. *Bioorganic Med. Chem.* **2019**, *27*, 2553–2571.
- (53) Vinh, N. B.; Drinkwater, N.; Malcolm, T. R.; Kassiou, M.; Lucantoni, L.; Grin, P. M.;

- Butler, G. S.; Duffy, S.; Overall, C. M.; Avery, V. M.; Scammells, P. J.; McGowan, S. Hydroxamic Acid Inhibitors Provide Cross-Species Inhibition of Plasmodium M1 and M17 Aminopeptidases. *J. Med. Chem.* **2019**, *62*, 622–640.
- (54) Lasonder, E.; Janse, C. J.; Van Gemert, G. J.; Mair, G. R.; Vermunt, A. M. W.; Douradinha, B. G.; Van Noort, V.; Huynen, M. A.; Luty, A. J. F.; Kroeze, H.; Khan, S. M.; Sauerwein, R. W.; Waters, A. P.; Mann, M.; Stunnenberg, H. G. Proteomic Profiling of Plasmodium Sporozoite Maturation Identifies New Proteins Essential for Parasite Development and Infectivity. *PLoS Pathog.* **2008**, *4*, e1000195.
- (55) Lasonder, E.; Ishihama, Y.; Andersen, J. S.; Vermunt, A. M. W.; Pain, A.; Sauerwein, R. W.; Eling, W. M. C.; Hall, N.; Waters, A. P.; Stunnenberg, H. G.; Mann, M. Analysis of the Plasmodium Falciparum Proteome by High-Accuracy Mass Spectrometry. *Nature* **2002**, *419*, 537–542.
- (56) Florens, L.; Washburn, M. P.; Raine, J. D.; Anthony, R. M.; Grainger, M.; Haynes, J. D.; Moch, J. K.; Muster, N.; Sacci, J. B.; Tabb, D. L.; Witney, A. A.; Wolters, D.; Wu, Y.; Gardner, M. J.; Holder, A. A.; Sinden, R. E.; Yates, J. R.; Carucci, D. J. A Proteomic View of the Plasmodium Falciparum Life Cycle. *Nature* **2002**, *419*, 520–526.
- (57) Lowther, W. T.; Matthews, B. W. Structure and Function of the Methionine Aminopeptidases. *Biochim. Biophys. Acta - Protein Struct. Mol. Enzymol.* **2000**, *1477*, 157–167.
- (58) Bradshaw, R. A.; Brickey, W. W.; Walker, K. W. N-Terminal Processing: The Methionine Aminopeptidase and N Alpha-Acetyl Transferase Families. *Trends Biochem. Sci.* **1998**, *23*, 263–267.

- (59) Zhang, P.; Nicholson, D. E.; Bujnicki, J. M.; Su, X.; Brendle, J. J.; Ferdig, M.; Kyle, D. E.; Milhous, W. K.; Chiang, P. K. Angiogenesis Inhibitors Specific for Methionine Aminopeptidase 2 as Drugs for Malaria and Leishmaniasis. *J. Biomed. Sci.* **2002**, *9*, 34–40.
- (60) Chen, X.; Xie, S.; Bhat, S.; Kumar, N.; Shapiro, T. A.; Liu, J. O. Fumagillin and Fumarranol Interact with *P. Falciparum* Methionine Aminopeptidase 2 and Inhibit Malaria Parasite Growth In Vitro and In Vivo. *Chem. Biol.* **2009**, *16*, 193–202.
- (61) Chen, X.; Chong, C. R.; Shi, L.; Yoshimoto, T.; Sullivan, D. J.; Liu, J. O. Inhibitors of *Plasmodium Falciparum* Methionine Aminopeptidase 1b Possess Antimalarial Activity. *Proc. Natl. Acad. Sci. U. S. A.* **2006**, *103*, 14548–14553.
- (62) Davies, H. M.; Nofal, S. D.; McLaughlin, E. J.; Osborne, A. R. Repetitive Sequences in Malaria Parasite Proteins. *FEMS Microbiol. Rev* **2017**, *41*, 923–940.
- (63) Calcagno, S.; Klein, C. D. N-Terminal Methionine Processing by the Zinc-Activated *Plasmodium Falciparum* Methionine Aminopeptidase 1b. *Appl. Microbiol. Biotechnol.* **2016**, *100*, 7091–7102.
- (64) Lu, J.; Chong, C. R.; Hu, X.; Liu, J. O. Fumarranol, a Rearranged Fumagillin Analogue That Inhibits Angiogenesis in Vivo. *J. Med. Chem.* **2006**, *49*, 5645–5648.
- (65) Miyahisa, I.; Sameshima, T.; Hixon, M. S. Rapid Determination of the Specificity Constant of Irreversible Inhibitors (Kinact/KI) by Means of an Endpoint Competition Assay. *Angew. Chemie - Int. Ed.* **2015**, *54*, 14099–14102.
- (66) Sutanto, F.; Konstantinidou, M.; Dömling, A. Covalent Inhibitors: A Rational Approach to Drug Discovery. *RSC Med. Chem.* **2020**, *11*, 876–884.

- (67) Rawlings, N. D.; Barrett, A. J.; Bateman, A. MEROPS: The Database of Proteolytic Enzymes, Their Substrates and Inhibitors. *Nucleic acids res* **2014**, *42*, D503–D509.
- (68) Florent, I.; Derhy, Z.; Allary, M.; Monsigny, M.; Mayer, R.; Schrével, J. A Plasmodium Falciparum Aminopeptidase Gene Belonging to the M1 Family of Zinc-Metallopeptidases Is Expressed in Erythrocytic Stages. *Mol. Biochem. Parasitol.* **1998**, *97*, 149–160.
- (69) Ragheb, D.; Dalal, S.; Bompiani, K. M.; Ray, W. K.; Klemba, M. Distribution and Biochemical Properties of an M1-Family Aminopeptidase in Plasmodium Falciparum Indicate a Role in Vacuolar Hemoglobin Catabolism. *J. Biol. Chem.* **2011**, *286*, 27255–27265.
- (70) McGowan, S.; Porter, C. J.; Lowther, J.; Stack, C. M.; Golding, S. J.; Skinner-Adams, T. S.; Trenholme, K. R.; Teuscher, F.; Donnelly, S. M.; Grembecka, J.; Mucha, A.; Kafarski, P.; Degori, R.; Buckle, A. M.; Gardiner, D. L.; Whisstock, J. C.; Dalton, J. P. Structural Basis for the Inhibition of the Essential Plasmodium Falciparum M1 Neutral Aminopeptidase. *Proc. Natl. Acad. Sci. U. S. A.* **2009**, *106*, 2537–2542.
- (71) Dalal, S.; Ragheb, D. R. T.; Schubot, F. D.; Klemba, M. A Naturally Variable Residue in the S1 Subsite of M1 Family Aminopeptidases Modulates Catalytic Properties and Promotes Functional Specialization. *J. Biol. Chem.* **2013**, *288*, 26004–26012.
- (72) Salomon, E.; Schmitt, M.; Mouray, E.; McEwen, A. G.; Bounaadja, L.; Torchy, M.; Poussin-Courmontagne, P.; Alavi, S.; Tarnus, C.; Cavarelli, J.; Florent, I.; Albrecht, S. Aminobenzosuberone Derivatives as PfA-M1 Inhibitors: Molecular Recognition and Antiplasmodial Evaluation. *Bioorg. Chem.* **2020**, *98*. DOI: 10.1016/j.bioorg.2020.103750.

- (73) Nocek, B.; Mulligan, R.; Bargassa, M.; Collart, F.; Joachimiak, A. Crystal Structure of Aminopeptidase N from Human Pathogen *Neisseria Meningitidis*. *Proteins Struct. Funct. Genet.* **2008**, *70*, 273–279.
- (74) Ito, K.; Nakajima, Y.; Onohara, Y.; Takeo, M.; Nakashima, K.; Matsubara, F.; Ito, T.; Yoshimoto, T. Crystal Structure of Aminopeptidase N (Proteobacteria Alanyl Aminopeptidase) from *Escherichia Coli* and Conformational Change of Methionine 260 Involved in Substrate Recognition. *J. Biol. Chem.* **2006**, *281*, 33664–33676.
- (75) Altschul, S. F.; Madden, T. L.; Schäffer, A. A.; Zhang, J.; Zhang, Z.; Miller, W.; Lipman, D. J. Gapped BLAST and PSI-BLAST: A New Generation of Protein Database Search Programs. *Nucleic acids res* **1997**, *25*, 3389–3402.
- (76) Chandu, D.; Nandi, D. PepN Is the Major Aminopeptidase in *Escherichia Coli*: Insights on Substrate Specificity and Role during Sodium-Salicylate-Induced Stress. *Microbiology* **2003**, *149*, 3437–3447.
- (77) Jones, P. M.; Robinson, M. W.; Dalton, J. P.; George, A. M. The *Plasmodium Falciparum* Malaria M1 Alanyl Aminopeptidase (PfA-M1): Insights of Catalytic Mechanism and Function from MD Simulations. *PLoS One* **2011**, *6*, e28589.
- (78) Allary, M.; Schrevel, J.; Florent, I. Properties, Stage-Dependent Expression and Localization of *Plasmodium Falciparum* M1 Family Zinc-Aminopeptidase. *Parasitology* **2002**, *125*, 1–10.
- (79) Rawlings, N. D.; Tolle, D. P.; Barrett, A. J. Evolutionary Families of Peptidase Inhibitors. *Biochem. J.* **2004**, *378*, 705–716.

- (80) Poreba, M.; McGowan, S.; Skinner-Adams, T. S.; Trenholme, K. R.; Gardiner, D. L.; Whisstock, J. C.; To, J.; Salvesen, G. S.; Dalton, J. P.; Drag, M. Fingerprinting the Substrate Specificity of M1 and M17 Aminopeptidases of Human Malaria, *Plasmodium Falciparum*. *PLoS One* **2012**, *7*, e31938.
- (81) Dalal, S.; Ragheb, D. R. T.; Klemba, M. Engagement of the S1, S1' and S2' Subsites Drives Efficient Catalysis of Peptide Bond Hydrolysis by the M1-Family Aminopeptidase from *Plasmodium Falciparum*. *Mol. Biochem. Parasitol.* **2012**, *183*, 70–77.
- (82) Niven, G. W.; Holder, S. A.; Strøman, P. A Study of the Substrate Specificity of Aminopeptidase N from *Lactococcus Lactis* Subsp. *Cremoris* Wg2. *Appl. Microbiol. Biotechnol.* **1995**, *44*, 100–105.
- (83) Chappellet-Tordo, D.; Lazdunski, C.; Murgier, M.; Lazdunski, A. Aminopeptidase N from *Escherichia Coli*: Ionizable Active-Center Groups and Substrate Specificity. *Eur. J. Biochem.* **1977**, *81*, 299–305.
- (84) Kumar, A.; Nandi, D. Characterization and Role of Peptidase N from *Salmonella Enterica* Serovar Typhimurium. *Biochem. Biophys. Res. Commun.* **2007**, *353*, 706–712.
- (85) Kuhn, Y.; Rohrbach, P.; Lanzer, M. Quantitative PH Measurements in *Plasmodium Falciparum*-Infected Erythrocytes Using PHluorin. *Cell. Microbiol.* **2007**, *9*, 1004–1013.
- (86) Klonis, N.; Tan, O.; Jackson, K.; Goldberg, D.; Klemba, M.; Tilley, L. Evaluation of PH during Cytostomal Endocytosis and Vacuolar Catabolism of Haemoglobin in *Plasmodium Falciparum*. *Biochem. J.* **2007**, *407*, 343–354.
- (87) Hayward, R.; Saliba, K. J.; Kirk, K. The PH of the Digestive Vacuole of *Plasmodium*

- Falciparum Is Not Associated with Chloroquine Resistance. *J. Cell Sci.* **2006**, *119*, 1016–1025.
- (88) Velmourougane, G.; Harbut, M. B.; Dalal, S.; McGowan, S.; Oellig, C. A.; Meinhardt, N.; Whisstock, J. C.; Klemba, M.; Greenbaum, D. C. Synthesis of New (-)-Bestatin-Based Inhibitor Libraries Reveals a Novel Binding Mode in the S1 Pocket of the Essential Malaria M1 Metalloaminopeptidase. *J. Med. Chem.* **2011**, *54*, 1655–1666.
- (89) Grembecka, J.; Mucha, A.; Cierpicki, T.; Kafarski, P. The Most Potent Organophosphorus Inhibitors of Leucine Aminopeptidase. Structure-Based Design, Chemistry, and Activity. *J. Med. Chem.* **2003**, *46*, 2641–2655.
- (90) Flipo, M.; Beghyn, T.; Leroux, V.; Florent, I.; Deprez, B. P.; Deprez-Poulain, R. F. Novel Selective Inhibitors of the Zinc Plasmodial Aminopeptidase PfA-M1 as Potential Antimalarial Agents. *J. Med. Chem.* **2007**, *50*, 1322–1334.
- (91) Flipo, M.; Florent, I.; Grellier, P.; Sergheraert, C.; Deprez-Poulain, R. Design, Synthesis and Antimalarial Activity of Novel, Quinoline-Based, Zinc Metallo-Aminopeptidase Inhibitors. *Bioorganic Med. Chem. Lett.* **2003**, *13*, 2659–2662.
- (92) Scornik, O. A.; Botbol, V. Bestatin as an Experimental Tool in Mammals. *Curr. Drug Metab.* **2001**, *2*, 67–85.
- (93) Umezawa, H.; Aoyagi, T.; Suda, H.; Hamada, M.; Takeuchi, T. Bestatin, an Inhibitor of Aminopeptidase B, Produced by Actinomycetes. *J. Antibiot. (Tokyo)*. **1976**, *29*, 97–99.
- (94) Nankya-Kitaka, M. F.; Curley, G. P.; Gavigan, C. S.; Bell, A.; Dalton, J. P. Plasmodium Chabaudi Chabaudi and P. Falciparum: Inhibition of Aminopeptidase and Parasite Growth

- by Bestatin and Nitrobestatin. *Parasitol. Res.* **1998**, *84*, 552–558.
- (95) González-Bacerio, J.; Maluf, S. E. C.; Méndez, Y.; Pascual, I.; Florent, I.; Melo, P. M. S.; Budu, A.; Ferreira, J. C.; Moreno, E.; Carmona, A. K.; Rivera, D. G.; Alonso del Rivero, M.; Gazarini, M. L. KBE009: An Antimalarial Bestatin-like Inhibitor of the Plasmodium Falciparum M1 Aminopeptidase Discovered in an Ugi Multicomponent Reaction-Derived Peptidomimetic Library. *Bioorganic Med. Chem.* **2017**, *25*, 4628–4636.
- (96) Syrén, P.-O. Enzymatic Hydrolysis of Tertiary Amide Bonds by Anti Nucleophilic Attack and Protonation. *J. Org. Chem.* **2018**, *83*, 13543–13548.
- (97) Loria, P.; Miller, S.; Foley, M.; Tilley, L. Inhibition of the Peroxidative Degradation of Haem as the Basis of Action of Chloroquine and Other Quinoline Antimalarials. *Biochem. J.* **1999**, *339*, 363–370.
- (98) Skinner-Adams, T. S.; Lowther, J.; Teuscher, F.; Stack, C. M.; Grembecka, J.; Mucha, A.; Kafarski, P.; Trenholme, K. R.; Dalton, J. P.; Gardiner, D. L. Identification of Phosphinate Dipeptide Analog Inhibitors Directed against the Plasmodium Falciparum M17 Leucine Aminopeptidase as Lead Antimalarial Compounds. *J. Med. Chem.* **2007**, *50*, 6024–6031.
- (99) Bounaadja, L.; Schmitt, M.; Albrecht, S.; Mouray, E.; Tarnus, C.; Florent, I. Selective Inhibition of PfA-M1, over PfA-M17, by an Amino-Benzosuberone Derivative Blocks Malaria Parasites Development in Vitro and in Vivo. *Malar. J.* **2017**, *16*. DOI: 10.1186/s12936-017-2032-4.
- (100) Maieranu, C.; Schmitt, C.; Schifano-Faux, N.; Le Nouën, D.; Defoin, A.; Tarnus, C. A Novel Amino-Benzosuberone Derivative Is a Picomolar Inhibitor of Mammalian

- Aminopeptidase N/CD13. *Bioorganic Med. Chem.* **2011**, *19*, 5716–5733.
- (101) Albrecht, S.; Al-Lakkis-Wehbe, M.; Orsini, A.; Defoin, A.; Pale, P.; Salomon, E.; Tarnus, C.; Weibel, J. M. Amino-Benzosuberone: A Novel Warhead for Selective Inhibition of Human Aminopeptidase-N/CD13. *Bioorganic Med. Chem.* **2011**, *19*, 1434–1449.
- (102) The PyMOL Molecular Graphics System, Version 2.0 Schrödinger, LLC.
- (103) Deprez-Poulain, R.; Flipo, M.; Piveteau, C.; Leroux, F.; Dassonneville, S.; Florent, I.; Maes, L.; Cos, P.; Deprez, B. Structure-Activity Relationships and Blood Distribution of Antiplasmodial Aminopeptidase-1 Inhibitors. *J. Med. Chem.* **2012**, *55*, 10909–10917.
- (104) Stack, C. M.; Lowther, J.; Cunningham, E.; Donnelly, S.; Gardiner, D. L.; Trenholme, K. R.; Skinner-Adams, T. S.; Teuscher, F.; Grembecka, J.; Mucha, A.; Kafarski, P.; Lua, L.; Bell, A.; Dalton, J. P. Characterization of the Plasmodium Falciparum M17 Leucyl Amino peptidase: A Protease Involved in Amino Acid Regulation with Potential for Antimalarial Drug Development. *J. Biol. Chem.* **2007**, *282*, 2069–2080.
- (105) McGowan, S.; Oellig, C. A.; Birru, W. A.; Caradoc-Davies, T. T.; Stack, C. M.; Lowther, J.; Skinner-Adams, T.; Mucha, A.; Kafarski, P.; Grembecka, J.; Trenholme, K. R.; Buckle, A. M.; Gardiner, D. L.; Dalton, J. P.; Whisstock, J. C. Structure of the Plasmodium Falciparum M17 Amino peptidase and Significance for the Design of Drugs Targeting the Neutral Exopeptidases. *Proc. Natl. Acad. Sci. U. S. A.* **2010**, *107*, 2449–2454.
- (106) Matsui, M.; Fowler, J. H.; Walling, L. L. Leucine Amino peptidases: Diversity in Structure and Function. *Biol. Chem.* **2006**, *387*, 1535–1544.
- (107) Burley, S. K.; David, P. R.; Taylor, A.; Lipscomb, W. N. Molecular Structure of Leucine

- Amino peptidase at 2.7-Å Resolution. *Proc. Natl. Acad. Sci. U. S. A.* **1990**, *87*, 6878–6882.
- (108) Maric, S.; Donnelly, S. M.; Robinson, M. W.; Skinner-Adams, T.; Trenholme, K. R.; Gardiner, D. L.; Dalton, J. P.; Stack, C. M.; Lowther, J. The M17 Leucine Amino peptidase of the Malaria Parasite *Plasmodium Falciparum*: Importance of Active Site Metal Ions in the Binding of Substrates and Inhibitors. *Biochemistry* **2009**, *48*, 5435–5439.
- (109) Carpenter, F. H.; Vahl, J. M. Leucine Amino peptidase (Bovine Lens). Mechanism of Activation by Mg<sup>2+</sup> and Mn<sup>2+</sup> of the Zinc Metalloenzyme, Amino Acid Composition, and Sulfhydryl Content. *J. Biol. Chem.* **1973**, *248*, 294–304.
- (110) Kim, H.; Lipscomb, W. N. Differentiation and Identification of the Two Catalytic Metal Binding Sites in Bovine Lens Leucine Amino peptidase by X-Ray Crystallography. *Proc. Natl. Acad. Sci. U. S. A.* **1993**, *90*, 5006–5010.
- (111) Carroll, R. K.; Veillard, F.; Gagne, D. T.; Lindenmuth, J. M.; Poreba, M.; Drag, M.; Potempa, J.; Shaw, L. N. The *Staphylococcus Aureus* Leucine Amino peptidase Is Localized to the Bacterial Cytosol and Demonstrates a Broad Substrate Range That Extends beyond Leucine. *Biol. Chem.* **2013**, *394*, 791–803.
- (112) Martin, R. E.; Kirk, K. Transport of the Essential Nutrient Isoleucine in Human Erythrocytes Infected with the Malaria Parasite *Plasmodium Falciparum*. *Blood* **2007**, *109*, 2217–2224.
- (113) Krugliak, M.; Zhang, J.; Ginsburg, H. Intraerythrocytic *Plasmodium Falciparum* Utilizes Only a Fraction of the Amino Acids Derived from the Digestion of Host Cell Cytosol for the Biosynthesis of Its Proteins. *Mol. Biochem. Parasitol.* **2002**, *119*, 249–256.

- (114) Skinner-Adams, T. S.; Peatey, C. L.; Anderson, K.; Trenholme, K. R.; Krige, D.; Brown, C. L.; Stack, C.; Nsangou, D. M. M.; Mathews, R. T.; Thivierge, K.; Dalton, J. P.; Gardiner, D. L. The Aminopeptidase Inhibitor CHR-2863 Is an Orally Bioavailable Inhibitor of Murine Malaria. *Antimicrob. Agents Chemother.* **2012**, *56*, 3244–3249.
- (115) Drinkwater, N.; Bamert, R. S.; Sivaraman, K. K.; Paiardini, A.; McGowan, S. X-Ray Crystal Structures of an Orally Available Aminopeptidase Inhibitor, Tosedostat, Bound to Anti-Malarial Drug Targets PfA-M1 and PfA-M17. *Proteins Struct. Funct. Bioinforma.* **2015**, *83*, 789–795.
- (116) Sivaraman, K. K.; Paiardini, A.; Sieńczyk, M.; Ruggeri, C.; Oellig, C. A.; Dalton, J. P.; Scammells, P. J.; Drag, M.; McGowan, S. Synthesis and Structure-Activity Relationships of Phosphonic Arginine Mimetics as Inhibitors of the M1 and M17 Aminopeptidases from *Plasmodium Falciparum*. *J. Med. Chem.* **2013**, *56*, 5213–5217.
- (117) Mistry, S. N.; Drinkwater, N.; Ruggeri, C.; Sivaraman, K. K.; Loganathan, S.; Fletcher, S.; Drag, M.; Paiardini, A.; Avery, V. M.; Scammells, P. J.; McGowan, S. Two-Pronged Attack: Dual Inhibition of *Plasmodium Falciparum* M1 and M17 Metalloaminopeptidases by a Novel Series of Hydroxamic Acid-Based Inhibitors. *J. Med. Chem.* **2014**, *57*, 9168–9183.
- (118) Drinkwater, N.; Vinh, N. B.; Mistry, S. N.; Bamert, R. S.; Ruggeri, C.; Holleran, J. P.; Loganathan, S.; Paiardini, A.; Charman, S. A.; Powell, A. K.; Avery, V. M.; McGowan, S.; Scammells, P. J. Potent Dual Inhibitors of *Plasmodium Falciparum* M1 and M17 Aminopeptidases through Optimization of S1 Pocket Interactions. *Eur. J. Med. Chem.* **2016**, *110*, 43–64.

- (119) McGowan, S.; Scammells, P.; Vinh, N.; Drinkwater, N.; Lee, J. Novel Aminopeptidase Inhibitors and Methods of Use. WO 2017/008101, 2017.
- (120) Sivaraman, K. K.; Oellig, C. A.; Huynh, K.; Atkinson, S. C.; Poreba, M.; Perugini, M. A.; Trenholme, K. R.; Gardiner, D. L.; Salvesen, G.; Drag, M.; Dalton, J. P.; Whisstock, J. C.; McGowan, S. X-Ray Crystal Structure and Specificity of the Plasmodium Falciparum Malaria Aminopeptidase PfM18AAP. *J. Mol. Biol.* **2012**, *422*, 495–507.
- (121) Chen, Y.; Farquhar, E. R.; Chance, M. R.; Palczewski, K.; Kiser, P. D. Insights into Substrate Specificity and Metal Activation of Mammalian Tetrahedral Aspartyl Aminopeptidase. *J. Biol. Chem.* **2012**, *287*, 13356–13370.
- (122) Teuscher, F.; Lowther, J.; Skinner-Adams, T. S.; Spielmann, T.; Dixon, M. W. A.; Stack, C. M.; Donnelly, S.; Mucha, A.; Kafarski, P.; Vassiliou, S.; Gardiner, D. L.; Dalton, J. P.; Trenholme, K. R. The M18 Aspartyl Aminopeptidase of the Human Malaria Parasite Plasmodium Falciparum. *J. Biol. Chem.* **2007**, *282*, 30817–30826.
- (123) Kafarski, P.; Lejczak, B. The Biological Activity of Phosphono- and Phosphinopeptides. In *Aminophosphonic and Aminophosphinic Acids, Chemistry and Biological Activity*; Kukhar, V. P., Hudson, H. R., Eds.; John Wiley & Sons, Ltd: Chichester, United Kingdom, 2000; pp 407–442.
- (124) Spicer, T.; Fernandez-Vega, V.; Chase, P.; Scampavia, L.; To, J.; Dalton, J. P.; Da Silva, F. L.; Skinner-Adams, T. S.; Gardiner, D. L.; Trenholme, K. R.; Brown, C. L.; Ghosh, P.; Porubsky, P.; Wang, J. L.; Whipple, D. A.; Schoenen, F. J.; Hodder, P. Identification of Potent and Selective Inhibitors of the Plasmodium Falciparum M18 Aspartyl Aminopeptidase (PfM18AAP) of Human Malaria via High-Throughput Screening. *J.*

*Biomol. Screen.* **2014**, *19*, 1107–1115.

- (125) Schoenen, F. J.; Whipple, D.; Baillargeon, P.; Brown, C. L.; Chase, P.; Ferguson, J.; Fernandez-Vega, V.; Hodder, P.; Mathew, R.; Neuenswander, B.; Porubsky, P.; Rogers, S.; Skinner-Adams, T.; Sosa, M.; Spicer, T.; To, J.; Tower, N. A.; Trenholme, K. R.; Wang, J.; Weiner, W. S.; Aubé, J.; Rosen, H.; White, E. L.; Gardiner, D. L.; Dalton, J. P. Inhibitors of the Plasmodium Falciparum M17 Leucine Aminopeptidase. In *Probe Reports from the NIH Molecular Libraries Program*; National Center for Biotechnology Information (US), 2013.
- (126) Baell, J. B. Observations on Screening-Based Research and Some Concerning Trends in the Literature. *Future Med. Chem.* **2010**, *2*, 1529–1546.
- (127) Cunningham, D. F.; O'Connor, B. Proline Specific Peptidases. *Biochim. Biophys. Acta - Protein Struct. Mol. Enzymol.* **1997**, *1343*, 160–186.
- (128) Simmons, W. H. Aminopeptidase P2. In *Handbook of Proteolytic Enzymes*; Rawlings, N. D., Salvesen, G., Eds.; Elsevier Ltd, 2013; Vol. 2, pp 1528–1532.
- (129) Drinkwater, N.; Sivaraman, K. K.; Bamert, R. S.; Rut, W.; Mohamed, K.; Vinh, N. B.; Scammells, P. J.; Drag, M.; McGowan, S. Structure and Substrate Fingerprint of Aminopeptidase P from Plasmodium Falciparum. *Biochem. J.* **2016**, *473*, 3189–3204.
- (130) Bazan, J. F.; Weaver, L. H.; Roderick, S. L.; Huber, R.; Matthews, B. W. Sequence and Structure Comparison Suggest That Methionine Aminopeptidase, Prolidase, Aminopeptidase P, and Creatinase Share a Common Fold. *Proc. Natl. Acad. Sci. U. S. A.* **1994**, *91*, 2473–2477.

- (131) Graham, S. C.; Bond, C. S.; Freeman, H. C.; Guss, J. M. Structural and Functional Implications of Metal Ion Selection in Aminopeptidase P, a Metalloprotease with a Dinuclear Metal Center. *Biochemistry* **2005**, *44*, 13820–13836.
- (132) Li, X.; Lou, Z.; Li, X.; Zhou, W.; Ma, M.; Cao, Y.; Geng, Y.; Bartlam, M.; Zhang, X. C.; Rao, Z. Structure of Human Cytosolic X-Prolyl Aminopeptidase: A Double Mn(II)-Dependent Dimeric Enzyme with a Novel Three-Domain Subunit. *J. Biol. Chem.* **2008**, *283*, 22858–22866.
- (133) Suda, H.; Takita, T.; Aoyagi, T.; Umezawa, H. The Structure of Bestatin. *J. Antibiot. (Tokyo)*. **1976**, *29*, 100–101.
- (134) Burley, S. K.; David, P. R.; Sweet, R. M.; Taylor, A.; Lipscomb, W. N. Structure Determination and Refinement of Bovine Lens Leucine Aminopeptidase and Its Complex with Bestatin. *J. Mol. Biol.* **1992**, *224*, 113–140.
- (135) Umezawa, H.; Aoyagi, T.; Suda, H.; Hamada, M.; Takeuchi, T. Bestatin, an Inhibitor of Aminopeptidase B, Produced by Actinomycetes. *J. Antibiot. (Tokyo)*. **1976**, *29*, 97–99.
- (136) Prechel, M. M.; Orawski, A. T.; Maggiora, L. L.; Simmons, W. H. Effect of a New Aminopeptidase P Inhibitor, Apstatin, on Bradykinin Degradation in the Rat Lung. *J. Pharmacol. Exp. Ther.* **1995**, *275*, 1136–1142.
- (137) Krishna, S.; Bustamante, L.; Haynes, R. K.; Staines, H. M. Artemisinins: Their Growing Importance in Medicine. *Trends Pharmacol. Sci.* **2008**, *29*, 520–527.
- (138) Kaushansky, A.; Mikolajczak, S. A.; Vignali, M.; Kappe, S. H. I. Of Men in Mice: The Success and Promise of Humanized Mouse Models for Human Malaria Parasite Infections.

- Cell. Microbiol.* **2014**, *16*, 602–611.
- (139) Panteleev, J.; Gao, H.; Jia, L. Recent Applications of Machine Learning in Medicinal Chemistry. *Bioorg. Med. Chem. Lett.* **2018**, *28*, 2807–2815.
- (140) Fleming, N. How Artificial Intelligence Is Changing Drug Discovery. *Nature* **2018**, *557*, S55-S57.
- (141) Cheng, A.; Diller, D. J.; Dixon, S. L.; Egan, W. J.; Lauri, G.; Merz, K. M. Computation of the Physio-Chemical Properties and Data Mining of Large Molecular Collections. *J. Comput. Chem.* **2002**, *23*, 172–183.
- (142) Strategic Advisory Group on Malaria Eradication. *Malaria Eradication: Benefits, Future Scenarios and Feasibility. A Report of the Strategic Advisory Group on Malaria Eradication.*; Geneva, 2020.

## Table of Contents Graphic

